The Structure and Dynamics of Ringed Galaxies. I. The Morphology of Galaxy Rings, and Statistics of Their Apparent Shapes, Relative Sizes, and Apparent Orientations with Respect to Bars

R. Buta – University of Texas at Austin

Citation of published version:

Buta, R. (1986): The Structure and Dynamics of Ringed Galaxies. I. The Morphology of Galaxy Rings, and Statistics of Their Apparent Shapes, Relative Sizes, and Apparent Orientations with Respect to Bars. *Astrophysical Journal Supplement Series,* vol. 61(p. 609). DOI: https://doi.org/10.1086/191126

THE ASTROPHYSICAL JOURNAL SUPPLEMENT SERIES, 61:609–630, 1986 August

THE STRUCTURE AND DYNAMICS OF RINGED GALAXIES. I. THE MORPHOLOGY OF GALAXY RINGS, AND STATISTICS OF THEIR APPARENT SHAPES, RELATIVE SIZES, AND APPARENT ORIENTATIONS WITH RESPECT TO BARS

R. BUTA
Mount Stromlo and Siding Spring Observatories, Research School of Physical Sciences, Australian National University
Received 1985 July 8; accepted 1985 December 5

ABSTRACT

This paper describes the results of a major new survey of ringed galaxies based on the UK Schmidt and ESO *B* Sky Survey films. Measurements of apparent diameters, axis ratios, and relative bar/ring position angles have been made for 1200 objects up to the time of this writing. The survey has been undertaken explicitly to explore in more detail than before the connection between rings and galactic orbital resonances. The large sample allows one to say the following:

1. Inner rings in barred (SB) and weakly barred (SAB) galaxies possess a wide range of intrinsic axis ratios. For SB galaxies the distribution of apparent axis ratios of inner rings in 204 objects favors a distribution of intrinsic axis ratios roughly uniformly spread in the range $q_0 = 0.60$–0.95. A similar range is found for SAB inner rings based on a sample of 147 objects. For nonbarred (SA) galaxies the distribution of apparent axis ratios of the inner rings in 119 objects definitely suggests that such rings are rounder on average than those in barred galaxies. The favored range of true shapes for them is $q_0 = 0.85$–1.0.

2. Outer rings in barred galaxies also possess a range of intrinsic axis ratios, although the range is narrower than for inner rings and the rings on average are less eccentric than inner rings. For SB galaxies the preferred range is $q_0 = 0.7$–1.0 as deduced from 242 objects, while for SAB and SA galaxies the range is $q_0 = 0.8$–1.0 as deduced from samples of 107 and 48 objects, respectively.

3. Nuclear rings and their analogs in SA, SAB, and SB spirals may, on average, be rounder than inner and outer rings. These very small rings are sometimes crossed by secondary bars which are significantly misaligned with the major axis of a primary bar or inner pseudoring.

4. The distribution of apparent relative bar/ring position angles for SB outer rings strongly suggests that such rings have *two* preferred intrinsic alignment modes with respect to bars: a dominant perpendicular mode *and* a parallel mode. The two modes are morphologically distinct, and examples can be found which show the presence of a double structure, i.e., both types of outer ring.

5. The distributions of apparent relative position angles between bars and inner rings in galaxies demonstrates that such structures are intrinsically aligned parallel to bars. This seems to be true regardless of the apparent bar strength (i.e., SB vs. SAB).

These observations provide strong support for the *resonance hypothesis* of the origin of these rings in normal galaxies. This hypothesis interprets rings as concentrations of stars and gas which have developed secularly near an orbital resonance with a bar or some kind of nonaxisymmetric perturbation in the mass distribution. In particular, *the recognition of two orthogonal modes of preferred alignment among the outer rings and pseudorings of SB galaxies provides strong evidence that these features are linked to the outer Lindblad resonance*. It is shown that the bar-forcing models of M. P. Schwarz currently provide the best account of many of the observed properties of real galaxy rings.

Subject heading: galaxies: structure

I. INTRODUCTION

Our understanding of the nature of the ringlike structures that are often visible in the light distribution of spiral and lenticular galaxies has recently received an impetus from several observational and theoretical studies. On the observational side, Kormendy (1979), de Vaucouleurs and Buta (1980*a*, *b*), Buta and de Vaucouleurs (1982, 1983*a*, *b*), and Pedreros and Madore (1981) have shown that inner-ring diameters are correlated with the mass and structure of the parent galaxy, and in particular the latter studies have confirmed the conclusion of de Vaucouleurs (1956) that such rings can be used as geometric extragalactic distance indicators. On the theoretical side, Schwarz (1979, 1981, 1984*a*, *b*, *c*, 1985; see also Simkin, Su, and Schwarz 1980) has constructed some very interesting models which demonstrate how gaseous ringlike structures can arise around the well-known dynamical Lindblad resonances because of the way a barlike perturbation in the mass distribution generates spiral structure in the gas and then rearranges the material in the disk.

Numerous studies prior to this work (see Kormendy 1982*a* for an extensive list of references) also recognized the role of bars and resonances in spiral arm development, but only in Schwarz's work is the connection between rings and resonances made especially clear. If real rings are linked to such orbital resonances, then they could be extremely useful probes of galactic dynamics if we could reliably identify which resonance is linked with a given ring. Then it may be possible to measure pattern speeds in galaxies directly. *The pattern speed of the bar is a fundamental unknown which is of great concern to density wave theorists*. This makes an observational study of the properties of galaxy rings more important and timely than ever before.

In this series of papers I shall describe the morphologic, metric, photometric, and kinematic properties of ringed galaxies. The present paper is concerned mainly with the physical insights about all types of rings which can be gained purely from their morphology and from statistical studies of their apparent shapes, relative sizes, and apparent orientations with respect to bars. Subsequent papers will deal with the photometric and kinematic properties of several representative examples (see Buta 1984*a* for preliminary discussions). Section II describes the basic philosophy of my approach to the subject, while § III describes the theoretical basis for the work in more detail. Section IV describes a major morphological survey designed for testing some aspects of the theory, the results of the survey being described in § V. Conclusions are presented in § VI.

II. PHILOSOPHY

The term "ring" as used here will refer to a class of structures found mainly in *normal* galaxies (de Vaucouleurs 1959). These structures have little or no bearing on the peculiar class of "ring" galaxies (Freeman and de Vaucouleurs 1974; Lynds and Toomre 1976; Theys and Spiegel 1976) or "polar rings" (Schweizer, Whitmore, and Rubin 1983; Katz and Richstone 1984 and references therein) which have been the subject of much recent research. In disk galaxies one can identify a hierarchy of these normal rings (in order of increasing *relative* size): (1) nuclear rings; (2) inner rings; and (3) outer rings. Nuclear rings are the very small structures that are often found in the centers of barred or weakly barred spirals; NGC 1097 (Sersic 1958) is the best known example. Inner rings are the luminous enhancements often observed around the bars of barred spirals (Curtis 1918) or within the spheroidal component of nonbarred spirals (de Vaucouleurs 1959; Sandage 1961). Good photographs of many examples of the phenomenon can be found in Sandage (1961, 1975), Kormendy (1979), Sandage and Brucato (1979), and de Vaucouleurs and Buta (1980*b*). Outer rings are the diffuse enhancements enveloping the main bodies of many lenticulars and early spirals. Recent quantitative studies of these kinds of rings have been made by de Vaucouleurs (1975), Schommer (1976), Kormendy (1979), Gallagher and Wirth (1980), and Buta (1984*a*).

In addition to "pure" nuclear, inner, and outer rings, defined to be distinct, closed enhancements, one can often find traces of each type of ring, that is, partial ring patterns of a spiral character. These are referred to as "pseudorings," and they are more common than the pure, closed rings (de Vaucouleurs 1963; de Vaucouleurs and Buta 1980*b*). Statistical evidence (de Vaucouleurs and Buta 1980*b*; see also Kormendy 1979) has indicated that rings and pseudorings are similar in absolute and relative size, and hence are probably related phenomena.

Last, rings as detected on photographs can be characterized in large part by a measure of the strength of the luminosity enhancement. This strength shows a very wide range, from subtle enhancements at the edge of a lens to intense, well-defined enhancements.

These properties of rings have led to at least three diverse viewpoints when interpreting the phenomenon. In the most conservative view, one classifies as rings only those features which are a perfectly closed, continuous enhancement with no sign of breaks due to a spiral character. This is adopted in the *Revised Shapley-Ames Catalog* (Sandage and Tammann 1981, hereafter RSA), and I will refer to it as the narrow (or restrictive) definition of rings. In this viewpoint many genuinely interesting and prominent pseudo–inner rings (e.g., in NGC 1433, NGC 3081, NGC 3185, and NGC 4274; the latter three are in the Hubble Atlas) that are only barely different from closed inner rings are classified as "s"-variety features because the inner ring is formed by a pair of tightly wrapped spiral arms. As a result, the RSA types underestimate the frequency of pseudorings [normally denoted (rs) and (R′) for inner- and outer-ring types, respectively]. The second viewpoint is less conservative and recognizes that rings represent a fairly continuous property of galaxies. This is depicted in a well-known cross section of the revised Hubble system (de Vaucouleurs and de Vaucouleurs 1964, hereafter RC1), and is referred to as the broad (or continuum) viewpoint. The third viewpoint augments the cells of the revised Hubble system by considering galaxies to be composed of a small number of "building blocks" such as bars, rings, lenses, spheroids, disks, and so on. This is adopted by Kormendy (1979) as a means of understanding possible secular evolution in barred galaxies, and it is referred to as the "distinct component" viewpoint.

In this series of papers I shall adopt the broad viewpoint. Then the ringlike features in galaxies such as NGC 1433, NGC 3081, NGC 3185, and NGC 4274 will be classified as (r) or (rs), and the outer spiral patterns in many barred galaxies will be recognized as pseudo–outer rings. Many of the features that I will use in my statistics therefore would not be recognized as rings in the RSA. The broad viewpoint looks at galaxy morphology as a continuous sequence of forms which can be represented with a three-dimensional volume of classification "cells." *The number of cells is not prohibitive*, and as de Vaucouleurs (1959, 1963) has demonstrated, 97% of all disk galaxies can be placed within the cells without being forced to fit into the system.

A seeming drawback of the broad viewpoint is that the cell boundaries are fuzzy. Transition cases are never hard to find, and there will sometimes be a tendency to recognize features which appear to be related to the ring phenomenon in better defined cases but which are so weak that they could simply be artifacts of poor resolution, photographic contrast, unfavor-

able tilt, or variations in the pitch angle of the spiral pattern. Kormendy (1981, 1982*a*) has also criticized the revised Hubble types for S0 galaxies in RC1, claiming that lenses are not recognized but are either ignored or simply denoted as inner rings (r). It is true that lenses have not been recognized with their own special symbol in RC1; however, the RC1 recognizes subtle enhancements at the edges of lenses as rings, which may not be so classified in more conservative viewpoints. The issue is then in part a question of ring amplitude. I shall take the criticism seriously in this series, but note that a ringlike enhancement on a decreasing background can look like a ring if strong, or like a shoulder or plateau (lens) if weak.

These minor drawbacks of the broad viewpoint are inconsequential for the purposes of studying rings because large numbers of objects have measurable features. The next section describes what morphological characteristics we might expect of rings if they are linked to galactic resonances, and § IV describes a major new survey of rings designed in part for testing this resonance hypothesis.

III. THE RESONANCE HYPOTHESIS OF GALAXY RINGS

Any statistical study of galaxy rings would benefit greatly from some understanding of the probable nature of the rings. The most promising theory links the rings to dynamical resonances where some aspect of the orbital motion is in step with the rotation rate of a bar or barlike distortion in the mass distribution. Ringlike patterns of gas can develop secularly near resonances due to the crossing of perturbed trajectories in the bar field. In these regions gas clouds collide and will initially form spiral shock fronts whose forms slowly change as a result of torques exerted by the bar. In time gas gathers into ringlike concentrations whose optical morphology, after star formation, can closely resemble the shapes and orientations of resonant periodic orbits in the bar field. Ring formation is expected to be a *natural* consequence of barred galaxy dynamics.

The models of Schwarz (1979, 1981) allow us to gain some idea of what kinds of properties we would expect resonance rings to have. These are based on a particle-orbit approach, and allow for dissipation through cloud-cloud collisions. The reader should refer to Schwarz (1981) for the details of these models and recognize that some of the aspects of the models (for example, the rate of ring formation) depend on details of the *n*-body code.

Figures 1*a*–1*d* illustrate gas density distributions for the Schwarz models most relevant to this paper. The first two represent models which have pattern speeds such that only the major resonances, corotation (CR) and the outer Lindblad resonance (OLR), exist. The models are identical in all but one respect. That in Figure 1*a* started with a distribution of particles which cut off sharply just inside the final position of OLR, while that in Figure 1*b* included an initial distribution which tapered off gradually across this resonance. The final particle distributions reflect an interesting difference which can be attributed to these initial conditions. In Figure 1*a* the particles have settled into a pseudoring-like structure which is oriented perpendicular to the bar. The angular momenta of individual particles in this ring tend to be less than that of a circular orbit exactly at OLR, and for convenience I will refer to the ring as an OLR^- type outer pseudoring. An important aspect of this kind of ring is the way the arms "return" or dip in to the ends of the bar, giving the galaxy a broad "figure eight" appearance. In contrast to this, the outer pseudoring which develops in Figure 1*b* is elongated parallel to the bar. In this case the arms make an almost complete circuit and intersect each other on the minor axis of the bar, i.e., they do not "return" to the ends of the bar. For convenience, I will refer to this kind of outer pseudoring as an OLR^+ type ring.

Schwarz (1981) attributes the development of the two different kinds of outer ring to the existence of two families of periodic orbits near the OLR. The family just inside the resonance tends to be oriented perpendicular to the bar and has the distinctive property that orbits can "dimple" at the long axis of the bar. The family just outside the resonance is oriented parallel to the bar and the orbits tend to be less eccentric and hence less prone to dimpling. An important finding that Schwarz made is that a fairly uniform gas distribution or a strong bar field gives rise to the parallel mode rather than the perpendicular, implying that we perhaps ought to expect that observed outer rings will usually be oriented parallel to bars. This is one prediction which can be tested with detailed statistics (§ V).

Figure 1*c* shows a model which is similar to that in Figure 1*a* except that the pattern speed is low. This gives rise to an inner Lindblad resonance (ILR) near the center and a structure reminiscent of an inner ring just inside CR. The near-resonant condition in the center leads to a very eccentric nuclear ring of gas aligned parallel to the bar. The inner ring in this model is made of particles whose angular momenta are similar to those of circular orbits just inside the inner second harmonic resonance, $2HR^-$. This is the most important of the ultraharmonic resonances which occur close to and inside CR. The four-part structure of the ring, with breaks near the minor axis, its slight elongation along the bar, and the attendant arm doubling, is due to the general properties of the orbits near $2HR^-$ (Schwarz 1984*c*), and some of these characteristics have been observed in real galaxies (Buta 1984*b*; Buta 1986, hereafter Paper II). Note that in none of Schwarz's simulations does a ring develop exactly *at CR*.

Figure 1*d* shows a model based on an "inverted isochrone potential" (Schwarz 1979; Simkin, Su, and Schwarz 1980) whose singularity at the center ensures that an ILR will exist for almost any pattern speed. As with the OLR, there are two major families of periodic orbits near the ILR, a parallel family predominant just outside and a perpendicular family just inside. The forcing of gas clouds along these orbits and the crossing of trajectories at the resonance can lead to an oval of gas which, at least initially, is obliquely aligned to the bar axis rather than parallel or perpendicular. The time evolution of the model is such that the nuclear oval contracts and at the same time changes its orientation to nearly perpendicular to the bar.

The models described here suggest that we could gain some important physical insights about the nature of galaxy rings by making statistical studies of their relative sizes, apparent shapes, and apparent orientations with respect to bars. The

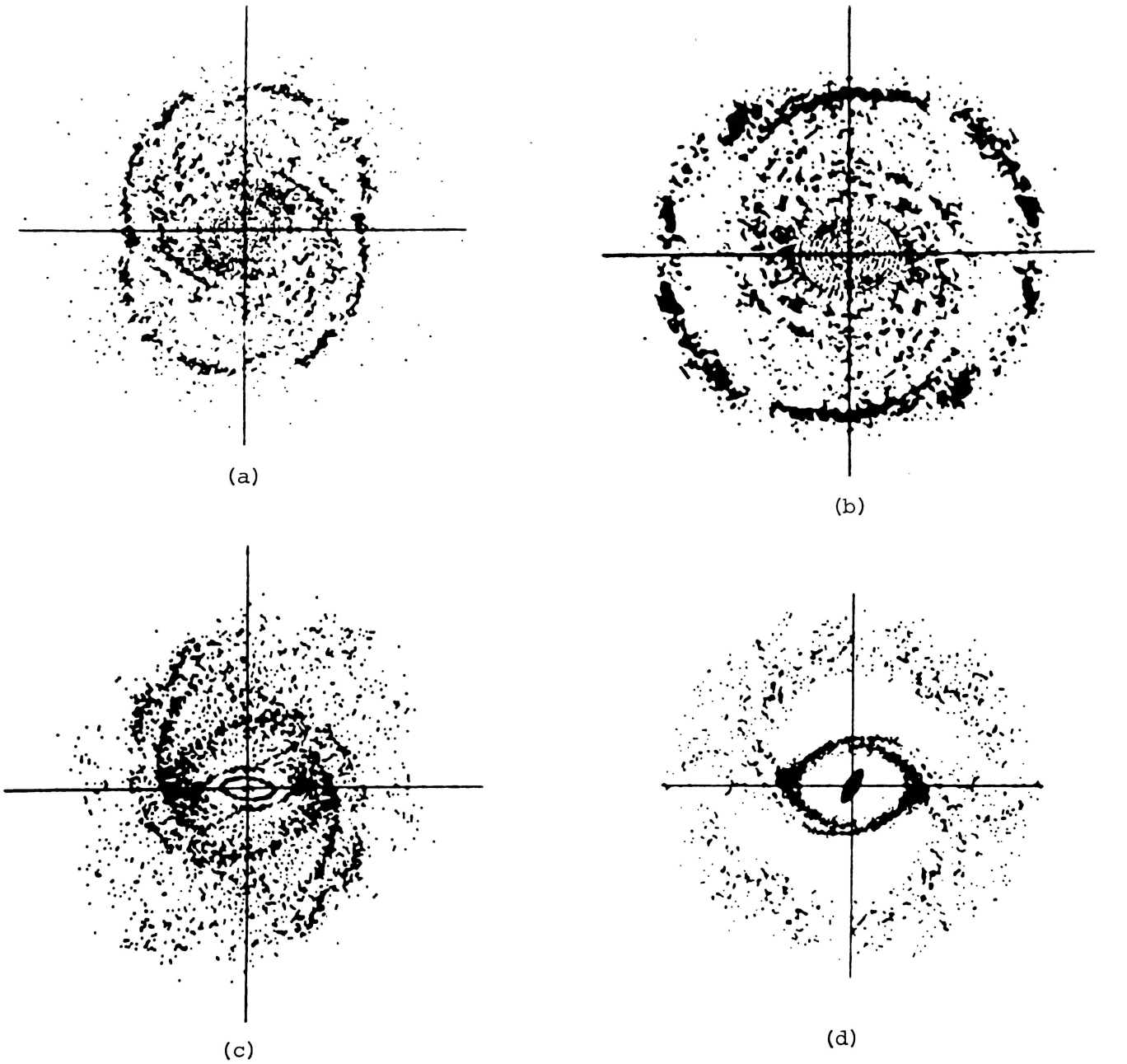

FIG. 1.—Gas density distribution plots from models by Schwarz (1979, 1981) which illustrate the possible morphological properties we might expect galactic resonance rings to have. Upper panels illustrate two types of outer pseudoring expected to occur close to the outer Lindblad resonance: (*a*) a type whose long axis is aligned perpendicular to the bar (OLR^-), and (*b*) a type whose long axis is aligned parallel to the bar (OLR^+). Lower panels illustrate some possible expected characteristics of rings which form close to corotation or to inner Lindblad resonance.

resonance hypothesis predicts, for example, that there should be preferred alignments between rings (at least of the inner and outer types) and bars, that rings should not be round, and that there should exist a hierarchy of ring types, since rings are expected to form near each of the three principal resonances: ILR, $2HR^-$, and OLR. More important, the shapes of pseudorings formed at OLR are predicted to be distinctive so that they could, in principle, be used to identify the location of this resonance. Finally, because of the relative homogeneity of the forms of galaxy rotation curves (rapid rise to maximum velocity, then constant velocity thereafter), we expect that the resonance radius ratio $r(\mathrm{OLR})/r(2\mathrm{HR}^-)$ will usually be very close to 2, but that the ratio $r(\mathrm{OLR})/r(\mathrm{ILR})$ will show much cosmic scatter, since galaxies differ most often in the form of the inner parts of the rotation curve, where ILR most likely will occur.

Some of these predictions have been tested (Athanassoula *et al.* 1982; Buta 1984*a*; Schwarz 1984*a*) using statistics based in part on a survey of 532 galaxies made by G. de Vaucouleurs during the 1950s (see de Vaucouleurs and

Buta 1980*a*, hereafter deVB). However, the deVB catalog is not entirely suited to testing the resonance hypothesis of the rings, for the following reasons. First, the catalog is seriously incomplete for all inner rings less than about 2′ in apparent diameter; hence in any given subcategory (e.g., restrictions by family or type) the samples will be small. Second, and most important, the catalog does not give values of relative bar/ring position angles which are critically needed for testing for preferred alignments between rings and bars (see Kormendy 1979 and Buta 1984*a* for these angles for many of the objects in deVB and Buta 1984*a* for a statistical application). Last, other interesting details concerning the character of the rings are not summarized in the catalog, although recognition of these details is important to interpreting the rings in terms of resonances.

IV. A MAJOR NEW SURVEY OF RINGED GALAXIES

One way of overcoming the limitations of the deVB catalog is to take advantage of the very high quality of the Science Research Council (SRC) J and European Southern Observatory (ESO) *B* sky surveys to search explicitly for all types of ringed galaxies. Rings as small as 0.2 mm in apparent size are both recognizable and measurable on the J films, and, more important, the original plates were sufficiently exposed to allow detection of very faint outer rings in an exceptionally large number of galaxies that would not be visible at all at the level of the Palomar Sky Survey. Also, one finds on these charts many excellent ringed systems not included in deVB, thereby allowing an opportunity to establish a very large, new sample of rings for statistics.

The principal objectives of the new survey are as follows:

1. To compile a large data base of measurements of diameters, axis ratios, and relative bar/ring position angles of inner, outer, and nuclear rings in 1500–2000 galaxies for definitive statistics to establish the intrinsic shapes and orientations of the structures with respect to bars.
2. To construct samples as complete as possible of *homogeneously* interpreted structures.
3. To look at the morphological structure of ringed galaxies with the models in Figure 1 in mind.
4. Possibly to identify or, better, to establish the existence of new phenomena such as "plumes" (Buta 1984*b*), secondary arms, or peculiar types of bars.

It is the author's intent to carry out the new survey of ringed systems over the complete set of 606 charts in the J sky survey, but at the time of this writing data have been collected only up to chart 365, excluding about 40 charts missing because of the incompleteness of the J survey. About 1200 objects have been measured thus far, enough for definitive statistics, but many excellent cases still remain unmeasured. The entire Catalog of Ringed Galaxies (hereafter RGC) will be published at a later date.

The survey has been carried out using a 7× Bausch and Lomb measuring magnifier having a scale divided into units of 0.1 mm. Measurements of ring major- and minor-axis dimensions were made as carefully as possible to the nearest 0.01 mm, while measurements of relative position angles were estimated to the nearest degree. Most measurements have been based only on the J films; however, for many galaxies the J films are overexposed in the inner regions. For these cases the ESO *B* films were used instead, and in general these films were referred to whenever the light distribution on a J film suggested the presence of an overexposed ring.

The precision of the new data can be judged by comparison with data given in Buta (1984*a*). For 48 objects in common I find good agreement on axis ratio measurements, the standard deviation about a line of unit slope being 0.052. This implies mean errors of $\sigma_q \approx 0.04$, although for very small rings ($d_r < 0.5$ mm) repeat measurements indicate larger errors ($\sigma_q \approx 0.06$). For 27 objects having measured relative bar/ring position angles I also find good agreement, the standard deviation about the line of unit slope being 5°.8. If the two data sets have equal errors, this indicates mean errors of about 4°, although for nearly round rings, foreshortened bars, highly inclined systems, or very small objects repeat measurements indicate larger errors ($\sigma_\theta \approx 7°$). A more detailed analysis of the internal and external errors of the new measurements will be given in the RGC.

In addition to the new measurements, detailed revised Hubble types were estimated for each object, but with several refinements:

1. To allow for large differences in amplitude, lenses have been distinguished from clear rings using notation (following Kormendy 1979) such as (l) for an inner lens (analog of inner rings), or (L) for an outer lens (analog of outer ring). Features with weak enhancements are variously denoted as (rl), (rl), or (rl) for inner lenses or (RL), and so on, for outer lenses.
2. Where unambiguously identifiable, nuclear rings will be recognized with the symbol (nr), and nuclear lenses with the symbol (nl). The small scale of the SRC J charts and problems with overexposure obviously mean that very few such structures could be detected in this survey.
3. In some galaxies, the form of the outer ring or pseudoring is very similar to one of the forms predicted by Schwarz in Figures 1*a* and 1*b*. Those rings or pseudorings which appear to be of the OLR^- type will be denoted R_1 or R'_1, respectively, while those which appear to be of the OLR^+ type will be denoted R_2 or R'_2. Figure 2 gives a basic schematic of the two types and in addition highlights a combined type to be discussed in the next section. Where no unambiguous identification can be made, the usual notations (R) or (R′) are used.
4. Details of the structure of the rings, arms, bars, and so on, not taken into account by the revised Hubble type are nevertheless treated as being of great importance and noted where possible. These details include (1) the quality (strength or definition) of a ring; (2) the shape or character of the inner ring, i.e., whether it is a closed oval, is broken at the minor-axis points of the bar, is rectangular or hexagonal or diamond-shaped, is made of wrapped spiral arms (i.e., arms which emerge from one end of the bar to cross the other), is of the "dash-dot-dash in brackets" type (de Vaucouleurs 1959), or which shows peculiar characteristics (e.g., ripples); (3) the character of the outer ring, whether it closes or remains fairly open, if it is broad or narrow, and so on; (4) the way the arms emerge from an (r), e.g., from the ends of the bar or from the ring on the minor axis of the bar; (5) the multiplicity of the outer spiral pattern; (6) a note on the size of the bar if the bar greatly underfills a ring, or if it greatly overextends across a

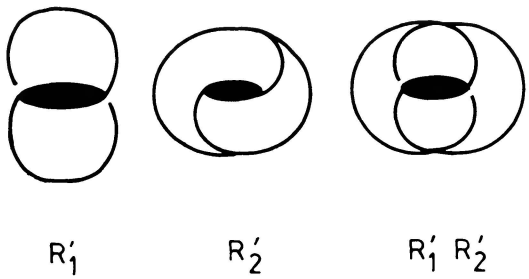

FIG. 2.—Schematic of observed morphologies of R'_1 and R'_2 outer pseudorings. Each type, as well as the combined type at right, is abundantly observed in nature. Real examples of each are shown in Figs. 3–5.

ring; (7) a note on the character of the bar; (8) a note if an object closely resembles a brighter, well-known object; and (9) a note on the presence or absence of "plumes" or any related secondary arms (Buta 1984*b*).

V. RESULTS FROM THE NEW SURVEY

a) *Morphology*

Examining a large number of galaxies with the objectives outlined in § IV provides a unique opportunity to view the full range of morphological possibilities among rings and bars. In this subsection I describe a few typical examples which best illustrate specific morphological properties, some of which will be taken into account in the detailed statistics. The statistical results for each ring type will be discussed separately in § V*b*.

i) *OLR$^+$ and OLR$^-$ Type Outer Rings and Pseudorings*

One of the most important results to come out of the survey is the recognition that there exist two distinct (and abundant) morphological subtypes among outer pseudorings whose statistical properties suggest that they are linked to the resonant orbits discussed by Schwarz. Figure 3 (Plate 35) illustrates six examples of R_1-type outer rings and pseudorings. Note how these all show the characteristic that arms emerge from each end of the bar and "return" to intersect the opposite end, as expected for pseudorings dominated by the OLR$^-$ class of resonant periodic orbits (refer to Fig. 1*a*). One of the objects, NGC 3504 (Fig. 3*e*), has been measured spectroscopically by Peterson (1982), who finds that, although the outer pseudoring appears nearly round, there is a significant measurable velocity gradient nearly along the axis of the bar. One way of explaining this is that the outer pseudoring is slightly elongated perpendicular to the bar, but, since the galaxy is tilted around the bar, the feature is foreshortened to appear almost circular.

In contrast to the objects in Figure 3, Figure 4 (Plate 36) shows six examples of R_2-type rings. Each of these objects has an outer pseudoring where the arms "return" to intersect nearly along the axis perpendicular to the bar, as expected for pseudorings dominated by the OLR$^+$ class of resonant orbits (refer to Fig. 1*b*).

Figure 5 (Plate 37) illustrates six interesting systems which show what I will refer to as the "($R'_1R'_2$) characteristic." In these cases the outer ring or pseudoring is complicated by what appears to be a double structure where, to some extent, both R_1 and R_2 subtypes can be recognized (see Fig. 2). One object, NGC 1291 (Fig. 5*a*), has long been recognized as showing faint spiral arms beyond its outer ring (de Vaucouleurs 1975), and I have placed it in this category for this reason. Only two of the objects, NGC 5701 (Fig. 5*b*) and A1340.6−2541 (Fig. 5*c*) are clear enough to be especially suggestive, while the others are weaker but obviously related cases. Is it possible that in these objects both the OLR$^+$ and the OLR$^-$ orbits are significantly populated? The interpretation seems plausible enough, but the coexistence of the two types of ring is something which has not been successfully simulated in numerical experiments. The models of Schwarz (1981) showed that only one of the main OLR orbits eventually dominates as the gas distribution evolves, the other being depleted by collisions. From inspection of nearly 600 outer rings I believe that there is a continuous sequence of forms between the R_1 and R_2 "cells," although the combined type with both components equally prominent (as appears to be the case in A1340.6−2541) is rare. It may be that in some galaxies the dissipation has not been effective enough to depopulate one of the main OLR-type orbits. However improbable the coexistence of the two types of ring may be on theoretical grounds, the six objects in Figure 5 do provide some food for thought.

In many galaxies the outer ring is not easily placed in either of these categories. Completely detached, closed rings showing no spiral character often will not show the requisite signatures (dimples, or intersecting arms). Even for some outer pseudorings, however, atypical emergence of the spiral structure from a bar or inner ring can make the structure unclassifiable in the context of current models. This means that refinement of these models will be needed at some point. More points concerning the details of the spiral structure in barred, ringed galaxies will be covered in the RGC.

Of course, some of the unclassifiable cases might involve outer rings or pseudorings which are not related to the OLR at all. Rings can form just inside CR (near 2HR$^-$, for example), but these would not be expected to have the same morphological appearance as those which form near OLR. Probable CR-type pseudorings are discussed in § V*a*(vi).

It is worth noting that many barred spirals display outer spiral patterns which are not even pseudoring-like in appearance. Some of these are illustrated in Figure 6 (Plates 38 and 39). In such cases it is possible that the OLR is too far out to have much influence on the inner regions, or that the effect of the bar has been too weak to significantly restructure the disks (Elmegreen and Elmegreen 1985). Alternatively, the outer spiral patterns may lie entirely within CR. Whatever the cause, barred spirals lacking outer pseudorings present somewhat of an enigma which future models should address.

ii) *Inner-Ring Morphologies*

Figure 6 shows that there is considerable variety in the morphology of inner rings. The best defined inner rings are completely or nearly closed ovals as in NGC 824 (Fig. 6*a*), but sometimes the ring is weak at the minor-axis points of the bar, giving it and the bar a "dash-dot-dash in brackets" appearance as in A1307.2−4610 (Fig. 6*b*). The inner ring of NGC 6782 (Fig 6*c*) is interesting in that it displays a slightly

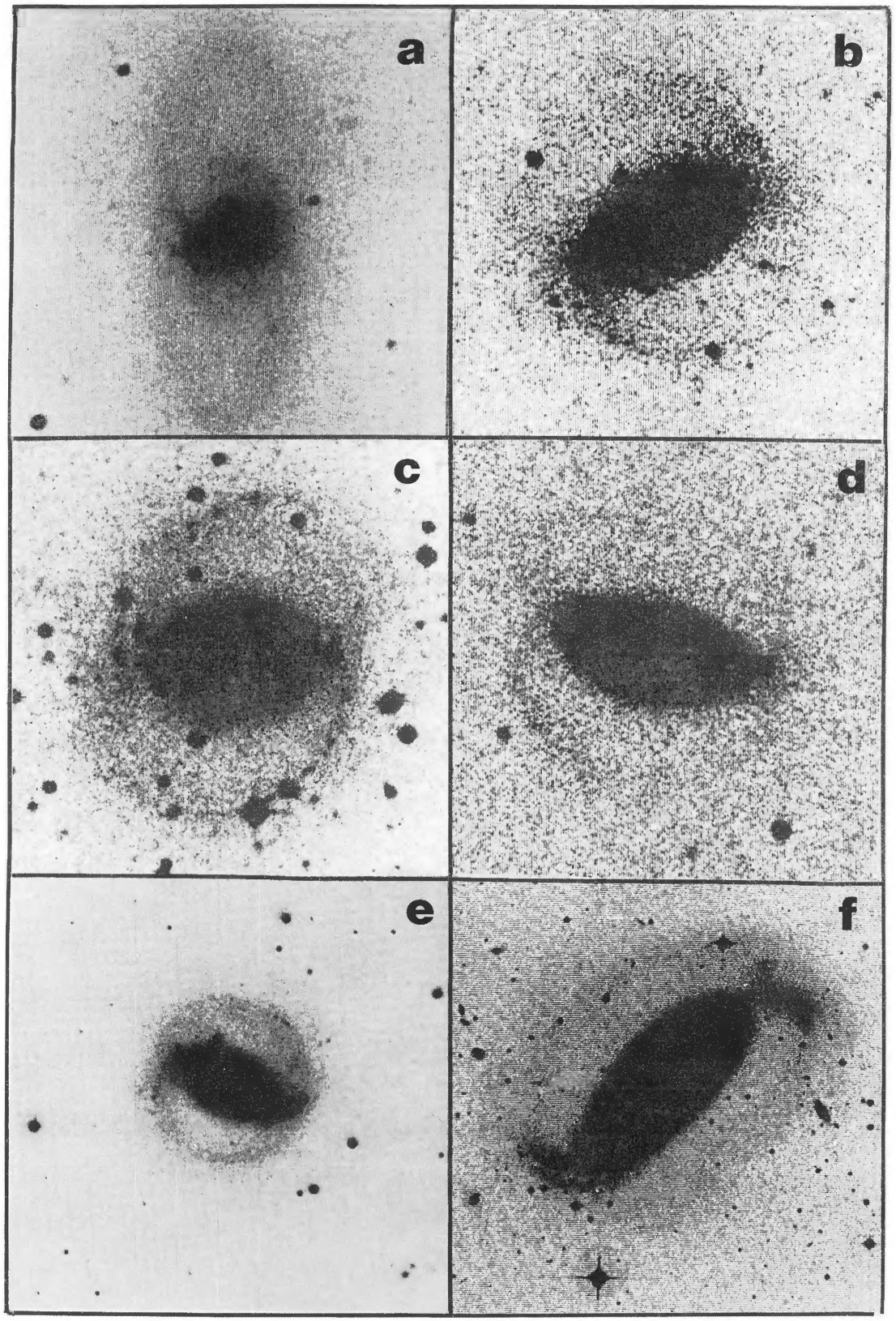

FIG. 3.—Examples of galaxies which show outer pseudorings of the R'_1 type: (*a*) A0243.7−5557; (*b*) A0134.8−8526; (*c*) NGC 6782 (*d*) A0106.7−3733; (*e*) NGC 3504; (*f*) NGC 1808. Except for NGC 3504 and 5701 (in Fig. 5), all images (including those in the successive figures) are based on scans with a PDS microdensitometer using a 5 μm square aperture at a sampling rate of 5 μm per step. Each was photographed from a RAMTEK display unit at suitably adjusted gray-scale levels. Orientations and scales are arbitrary. The photograph of NGC 3504 is from the Hubble Atlas, while that of NGC 5701 is from Kormendy (1979).

BUTA (*see* page 614)

PLATE 36

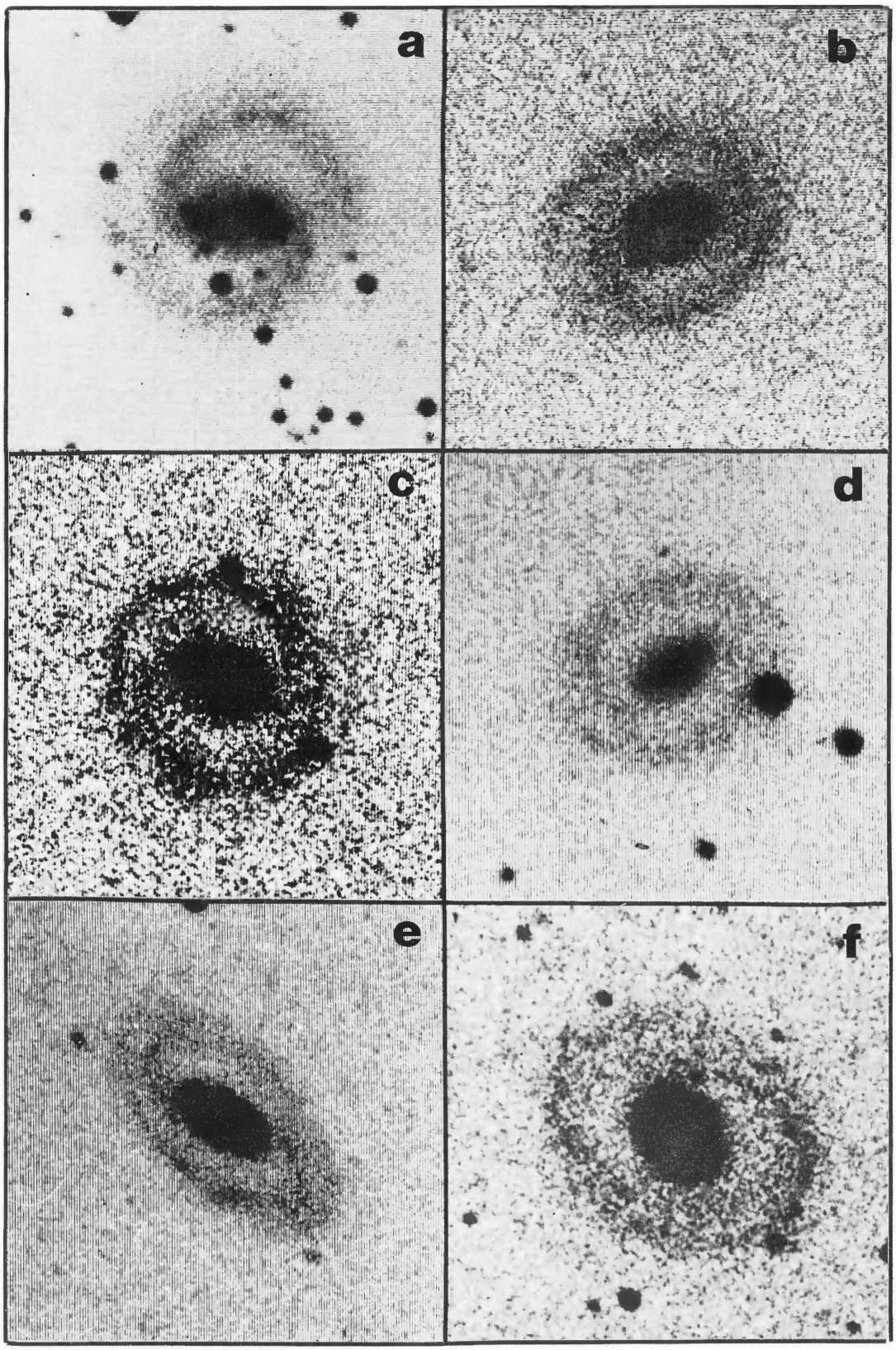

FIG. 4.—Examples of galaxies which show outer pseudorings of the R'_2 type: (*a*) A1347.7−3812; (*b*) A0139.5−4628; (*c*) A2341.6−3827; (*d*) A2035.8−4122; (*e*) A0024.7−4116; (*f*) A0635.0−3502.

BUTA (*see* page 614)

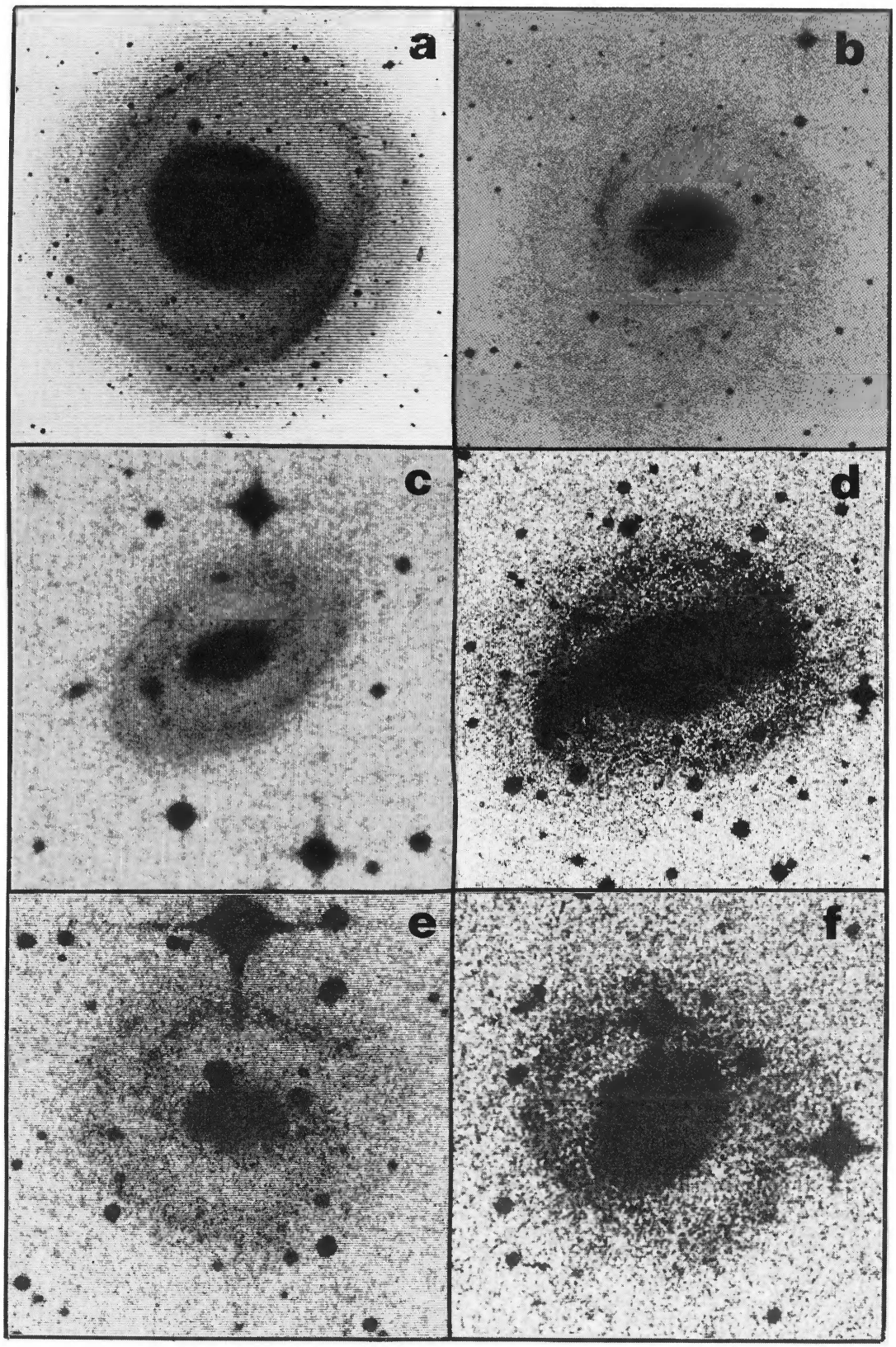

FIG. 5.—Examples of galaxies showing the "$(R'_1R'_2)$ characteristic": (*a*) NGC 1291; (*b*) NGC 5701; (*c*) A1340.6−2541; (*d*) A1056.3−4619; (*e*) A1116.4−4624; (*f*) A0621.9−3211.

BUTA (*see* page 614)

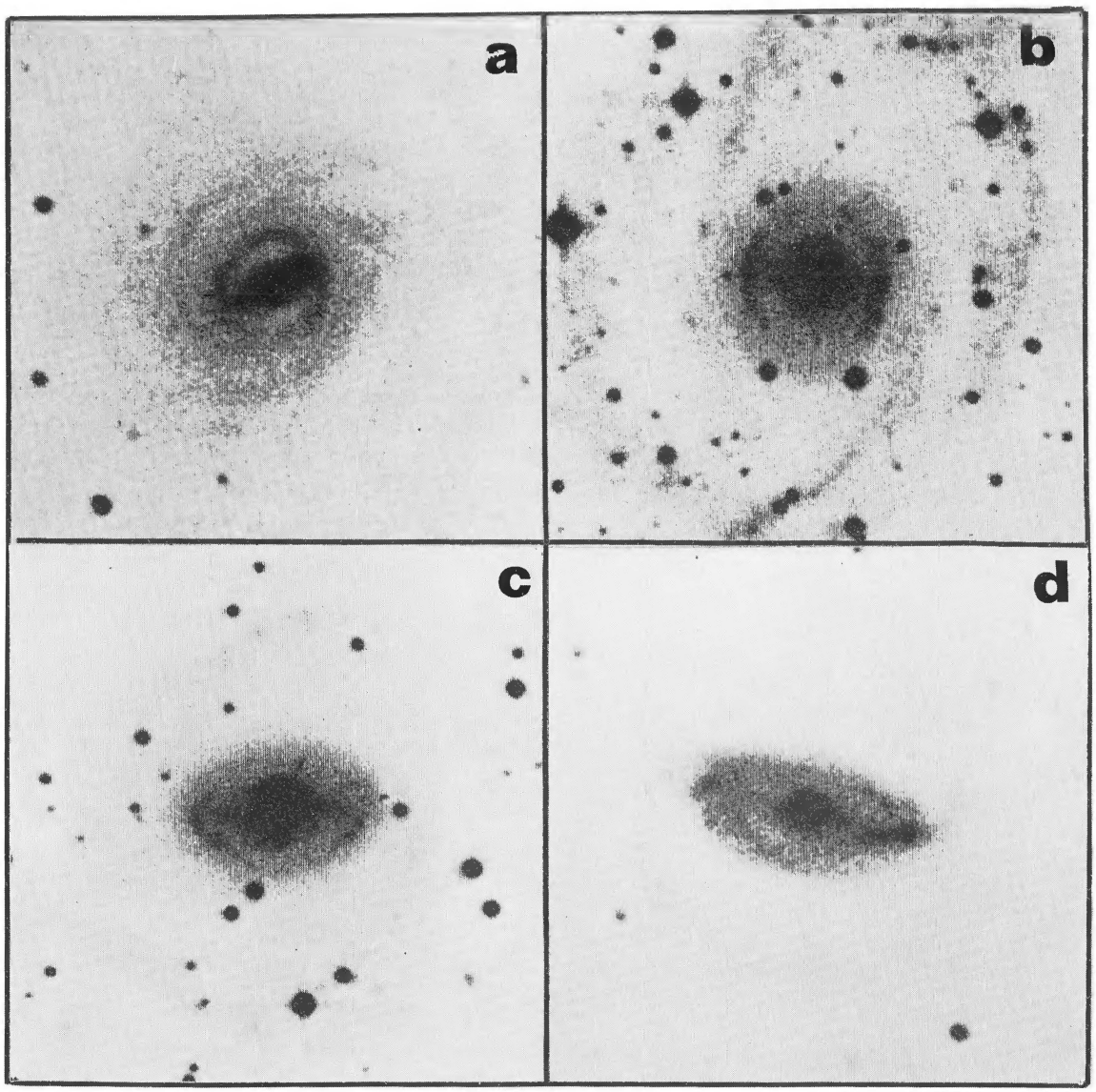

FIG. 6.—Examples of SB galaxies illustrating different inner-ring morphologies: (*a*) NGC 824 (closed circle); (*b*) A1307.2−4610 ("dash-dot-dash-in brackets" type); (*c*) NGC 6782 (pointed oval); (*d*) A0106.7−3733 (made of tightly wrapped spiral arms); (*e*) A0255.8−3655 (tilted rectangle); (*f*) NGC 3313 (broken at minor axis with segmented structure); (*g*) NGC 7020 (hexagonal type); (*h*) IC 4938 (open spiral type).

BUTA (*see* page 614)

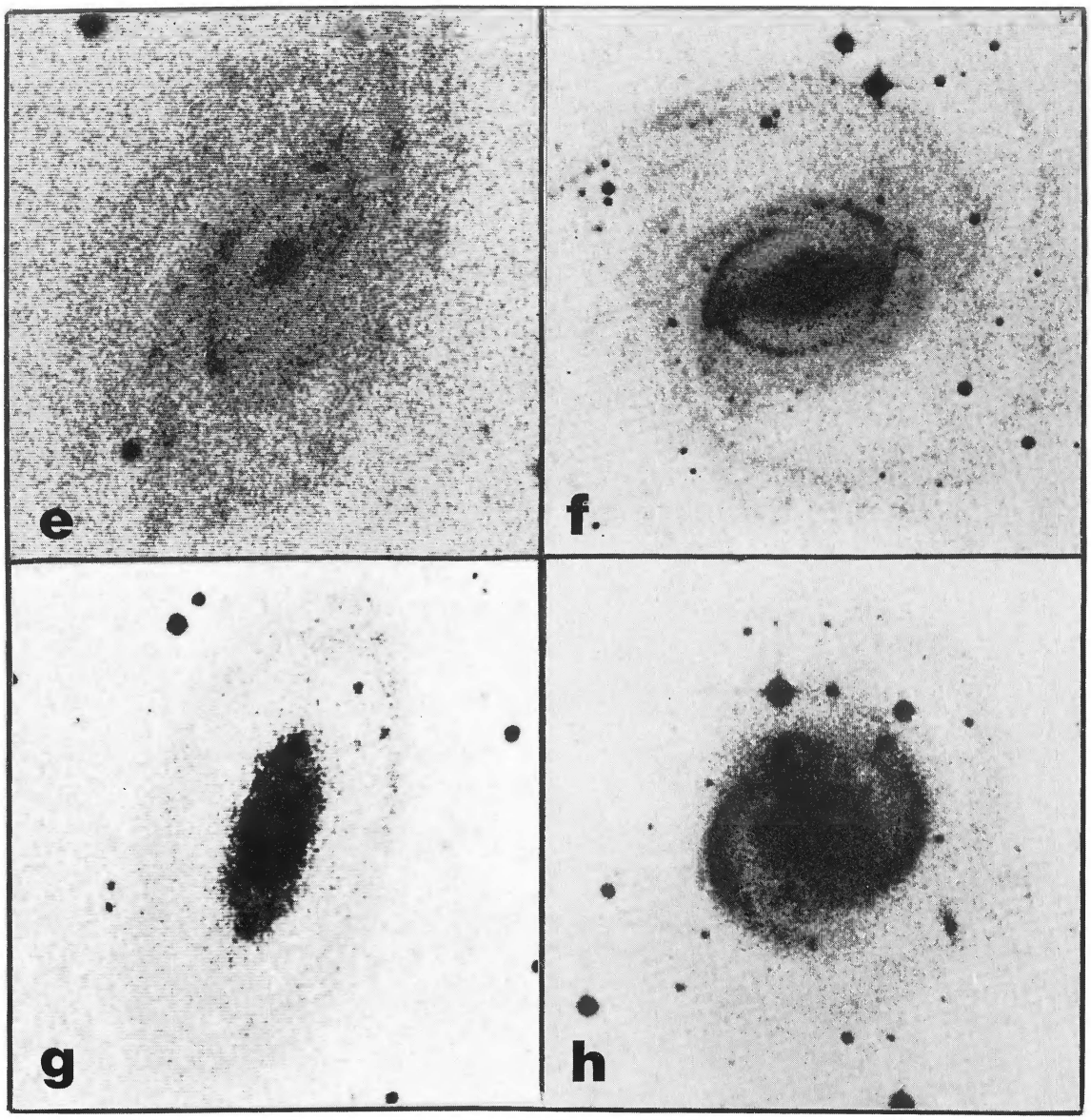

FIG. 6—*Continued*

BUTA (*see* page 614)

pointed oval shape (compare with the shape of the outer disk shown in Fig. 3*c*), while Figure 6*d* shows the inner regions of A0106.7−3733 (see also Fig. 3*d*), where an inner ring appears to be made of two tightly wrapped spiral arms. Some inner rings display sharp corners, as in A0255.8−3655 (Fig. 6*e*), where the inner ring seems to be a tilted rectangle, or in NGC 7020 (Fig. 6*g*), where the inner ring shows a clear *hexagonal* shape (this interesting object will be highlighted in a successive paper). De Vaucouleurs (1959, 1963) has emphasized how the inner rings and pseudorings in SAB spirals tend to show a *characteristic* hexagonal shape.

Figure 6*f* shows an interesting case (NGC 3313) where the striking inner ring displays a strong break on one side of its minor axis. As with the inner ring of NGC 1433 (to be described in Paper II) and several others illustrated in the Hubble Atlas, the ring of NGC 3313 can be thought of as being made of separate segments which do not quite match at the minor-axis zone of the bar, although the match seems good on the lower half of the structure. Referring to Figures 1*c* and 1*d*, we may infer that breaks in a ring at the minor-axis points of the bar could be a signature that the feature is linked with $2HR^-$. Many SB rings do not display such breaks, however, which may signify that some are not linked with $2HR^-$, although it is possible that as the ring evolves, the breaks will eventually close. This is suggested by the time sequence for Figure 1*d* shown by Simkin, Su, and Schwarz (1980).

Figure 6*h* shows an interesting case (IC 4938) where a closed outer ring surrounds an open spiral inner pseudoring of very high surface brightness. The pseudoring envelopes a weak bar and comes nowhere near to closing, yet it is distinct from the outer ring. It is clearly different from the spiral-like ring in A0106.7−3733.

iii) *Bar and Oval Morphologies*

One fact which becomes obvious from a large survey of ringed systems is the great variety in the morphology of nonaxisymmetric components in galaxies. One can recognize at least five distinct types of bar or barlike features, all of which have been known for some time: (1) "Saturn" or sliver bars, (2) "cigar" bars, (3) "three-blob" (or three-body) bars, (4) "ring/lens" barlike distortions, and (5) "spiral" barlike distortions.

The "Saturn" or sliver type of bar refers to the combined appearance of a bulge or spheroidal component from which two extensions or slivers emerge at diametrically opposite points, giving an impression reminiscent of a nearly edge-on view of Saturn and its rings. The Hubble Atlas illustrates many examples, some of the best being NGC 1398, NGC 2217, NGC 2523, and NGC 4394. A good case is shown here in Figure 8*b*.

A cigar bar is simply one which shows no fattening in the center. Such bars appear frequently in late-type spirals where the bulge is very small. In the Hubble Atlas, NGC 7741 and NGC 1073 are two late-type systems having very good cigar bars, while NGC 1317 is one good early-type example (see Fig. 8*c*). "Saturn" and "cigar" bars may differ not only in the amount of bulge. Elmegreen and Elmegreen (1985) showed that late-type galaxy bars and early-type galaxy bars tend to have very different luminosity profiles and may extend to different resonances. They suggested that early- and late-type galaxy bars could have been built up in different ways.

A "three-blob" bar is one type commonly found in barred lenticulars or early spirals. It consists of a bulge or spheroidal component flanked on opposite sides by two large secondary masses rather than just slivers of light. One of the best examples, NGC 2859, is illustrated in the Hubble Atlas, while an interesting case from my survey is shown in Figures 7*c* and 7*d* (Plate 40). The possible nature of this type of bar was first discussed by Danby (1965).

In some galaxies one observes a bulge enveloped by an oval lens or ring, but no slivers cross the ring as in a typical SB(r)-type spiral, or else only very weak slivers are observed. In many of these galaxies one observes an outer ring or pseudoring just like those observed in SB galaxies, and, more important, when the disk appears face-on these ring/lens structures are often highly elongated. In these cases the ring/lens must be the analog of a normal SB-type bar. Two interesting examples of this phenomenon which I found in my survey are illustrated in Figures 7*a*, 7*e*, and 7*f*. In the first (known as A1150.7−3851) there is a clear lens surrounding the bulge which is weakly enhanced at the edge; more significant enhancements are found at diametrically opposite points on the ring/lens, which could signify that a weak "three-blob" bar is present. In the second case (NGC 619) the ringlike enhancement at the edge of the lens is fairly intense, and could be made of spiral structure emerging directly from the bulge. The variety in the ring/lens "bar" morphology is further illustrated with several examples in the Hubble Atlas, these being NGC 210, NGC 1097, and NGC 3504.

An interesting and well-known type of "bar" that may be fairly common is the "spiral" bar, where a bright spiral pattern appears distributed within an oval distortion or oval lenslike region. The best known cases are NGC 1566 (de Vaucouleurs 1973; Simkin, Su, and Schwarz 1980) and NGC 5248; the former is shown in Figure 7*b*, while the latter is illustrated in the Hubble Atlas. In NGC 1566 a very bright spiral pattern emerges from a small round core, and then changes pitch angle and surface brightness some distance out to form an outer pseudoring which appears to be mainly of the R'_1 type. The same occurs in NGC 5248, except that the inner spiral pattern is more open. An interesting property of NGC 5248 is that it posses a bright oval nuclear ring of H II regions similar to the rings observed in barred spirals. From the morphology of these systems there is every reason to believe that the spiral bar is a subset of the ring/lens bars. In fact, NGC 619 may be a transition case between the two types.

Note that bars as defined by Hubble's classification system usually encompass only the first three categories (the SB types). The last two categories are more properly referred to as oval distortions, as has been recognized for some time. The discussion here is from a more global viewpoint, since conventional bars and mild oval distortions can lead to the formation of similar rings and pseudorings (Kormendy 1982*a* and references therein).

iv) *Inner-Ring Size and Bar Extent*

No cases have yet been found where a bar appears to overextend a well-defined ring, but there are frequent cases

PLATE 40

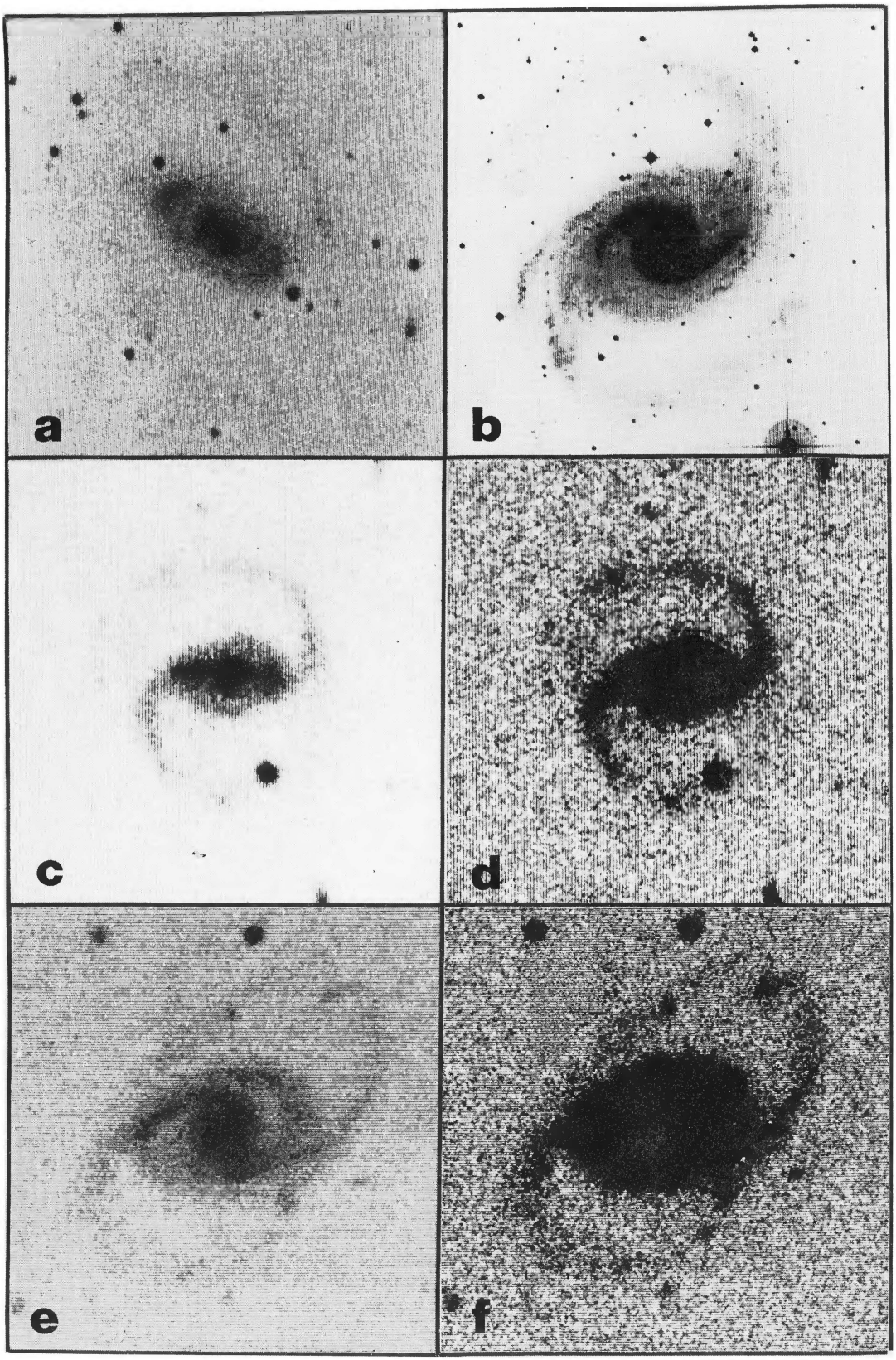

FIG. 7.—Examples of different bar/oval morphologies: (*a*) A1150.7−3851 (ring/lens bar); (*b*) NGC 1566 ("spiral" bar); (*c*) A0431.3−3326 ("three-blob" bar); (*d*) A0431.3−3326, to emphasize outer pseudoring (R'_1 type); (*e*) NGC 619 (ring/lens/spiral bar type); (*f*) NGC 619, to emphasize outer ring (R_1 type).

BUTA (*see* page 615)

where a bar appears to significantly underextend an inner ring. Nearly 30 cases have been found in the survey thus far, three of which are illustrated in Figure 8 (Plate 41). The first (A0253.8−7258, Fig. 8*a*) shows a weak inner ring which includes a rather stubby but clear bar. It is typical of most of the examples found. The second object (A0601.4−5837), shown in Figure 8*b*, includes a well-defined "Saturn" bar which slightly underfills the virtually closed inner ring. Figure 8*c* shows NGC 1317, where it is seen that the rather fat "cigar" bar underfills a circular lens enhanced at its edge. Two arms actually emerge from this zone to form a very faint outer ring.

Only about half of the objects in this category were found to have outer rings or pseudorings. In many cases only one ring is observed, and this ring marks the edge of the visible disk (little or no outside structure). This could signify that these rings are actually outer rings, in which case the bar would be expected to underfill the ring. However, these structures typically do not have the morphology of conventional outer rings in terms of surface brightness or character, hence this interpretation is quite uncertain. Many cases were in fact found where a bar exactly filled a ring, yet no outer structure was apparent. It is probable that, because of foreground Galactic extinction or intrinsic faintness, some outer rings or outer disks are lost, yet the high surface brightness inner rings remain apparent. Also, genuine cases are observed where a well-defined two-armed spiral pattern emerges from an underfilled ring. It thus appears that bars are not linked one-to-one with the size of an inner ring. Since more than one bar can exist in the same galaxy (next section), it is possible that in at least some of the objects in this category the bar simply extends to a different resonance compared with those where the bar fills the ring.

v) *Systems with Two Bars and the Case for a Bar Hierarchy*

Some objects are known to display two clear bars in the light distribution. NGC 1291 (de Vaucouleurs 1974, 1975) and NGC 1433 (Buta 1984*a*, *b*; Paper II) are two large, nearby examples, and many other cases are described by Kormendy (1979, 1982*b*). One interesting case from my survey, NGC 1317, was discussed in the previous section. The main cigar bar in this galaxy includes a secondary bar which crosses and underfills a small *nuclear ring* (Fig. 8*d*; see also Schweizer 1980). A striking characteristic is that the two bars are almost exactly perpendicular to each other. In NGC 1291 the two bars are misaligned by 30°, while in NGC 1433 they are misaligned by 62°. De Vaucouleurs (1975) has pointed out several other similar cases and has emphasized the frequent occurrence of misalignment (see also Kormendy 1982*a*, *b*; Buta 1984*a*). The bars also usually always have greatly different extents.

The cause of two bars in a system may be the existence of highly elongated orbits associated with an ILR. Between CR and the ILR the periodic orbits align along a bar, but inside the ILR these orbits are expected to be perpendicular to the bar, which could lead to a secondary oval misaligned with the primary bar (as illustrated by the Schwarz model in Fig. 1*d*). The fact that these secondary bars are occasionally enveloped by nuclear rings further argues for a link with the ILR. Cases showing the "nuclear spiral" phenomenon (e.g., NGC 4314; Sandage 1961) may be similarly linked. Other aspects of the dynamics of triaxial SB bulges discussed by Kormendy (1982*b*) provide strong support for a similarity between secondary and ordinary bars. The secondary bars in these objects will be referred to as "nuclear" bars.

vi) *Three-Ring or Three-Zone Nonbarred or Weakly Barred Galaxies*

Many barred spirals have two rings or pseudorings. Occasionally this combination of an inner and an outer ring is augmented by a central or nuclear ring or lens (e.g., NGC 1433).

Some nonbarred spirals also show a triple ring structure, or at least a "three-zone" structure which is analogous to the barred spirals (Sandage 1961; de Vaucouleurs 1975; Kormendy 1979; Simkin, Su, and Schwarz 1980). Most often they are just pseudorings formed by a spiral pattern, but a hierarchical aspect of the structures is identifiable (Buta 1984*a*; see also § V*c*). Four examples are illustrated in Figure 9 (Plates 42 and 43). One of these (NGC 6753, Fig. 9*a*) probably has a "spiral" bar. NGC 7637 (Fig. 9*b*) would be recognized as an ordinary spiral on underexposed plates, but the deep J films show an extensive envelope around this tight inner spiral zone that, although not very ringlike, is still very much reminiscent of the outer structure of NGC 6753.

Figures 9*c* and 9*d* show an unusual case, NGC 3783, where the inner ring is crossed by a clear "Saturn" bar from which two arms emerge to form an intermediate pseudoring (see also Simkin, Su, and Schwarz 1980). The presence of a very faint ringlike feature beyond this zone suggests that the brighter arms in NGC 3783 are not linked with the OLR orbits. This is one case which, in my opinion, does not fit well into the framework of the Schwarz models.

Figures 9*e*–9*f* show a definitive example where the three features are more ringlike than in the others. This is A0227.5−4843, and it displays a small nuclear ring enveloped by a detached intermediate ring which is peculiar in the sense of being doubled. The doubling is apparently caused by a very tight spiral pattern, and a similar phenomenon is observed in NGC 4725 (see photo in the Hubble Atlas). Surrounding the intermediate ring/spiral zone is a very faint and detached outer ring oriented nearly along the same position angle. No bar is evident within the intermediate ring.

The main point to note about these galaxies is that each has an "intermediate" zone between two fairly well-defined rings which has a fairly sharp edge, either lenslike or ringlike. It is hard to present an entirely convincing case for an analogy (i.e., same resonance types) for the features observed in these galaxies with those in barred spirals, but the analysis of ring ratios described in § V*c* suggests that the analogy may not be far wrong. Even if it is wrong, these galaxies represent a distinct class of object.

As will be demonstrated in § V*c*, the hierarchical aspect of the rings or pseudorings in these systems, their differing morphologies, and their differing relative frequencies are not adequately taken into account by the revised Hubble system. For this reason I will adopt the following notations where necessary: r_1 will refer to the smallest rings in the three-ring

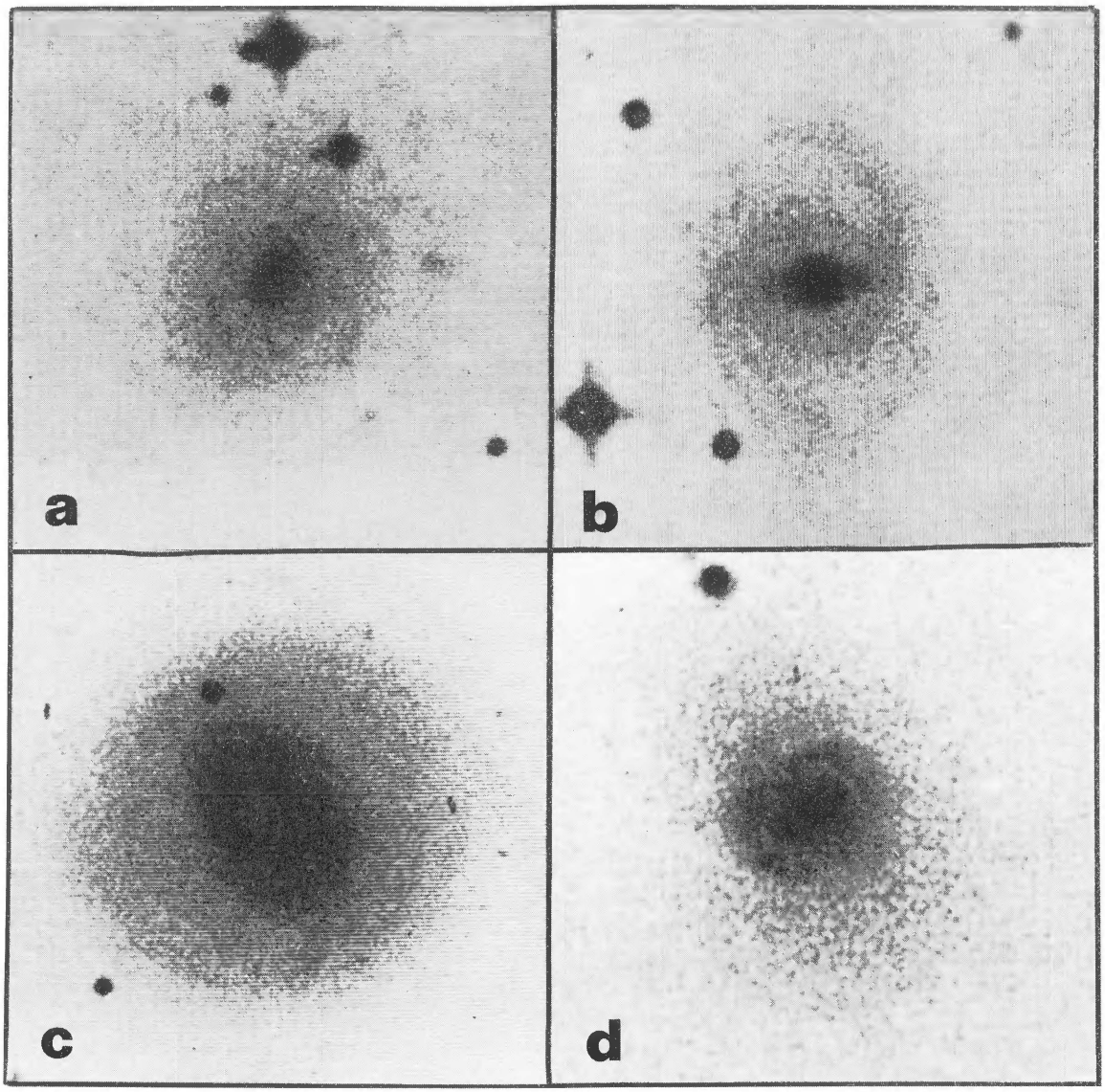

FIG. 8.—Three examples of galaxies where it appears that an inner ring is underfilled by a bar: (*a*) A0253.8−7258; (*b*) A0601.4−5837 (note prominent "Saturn" bar); (*c*) NGC 1317, to emphasize intermediate zone and "cigar" bar; (*d*) NGC 1317, to emphasize nuclear ring and bar.

BUTA (*see* page 616)

PLATE 42

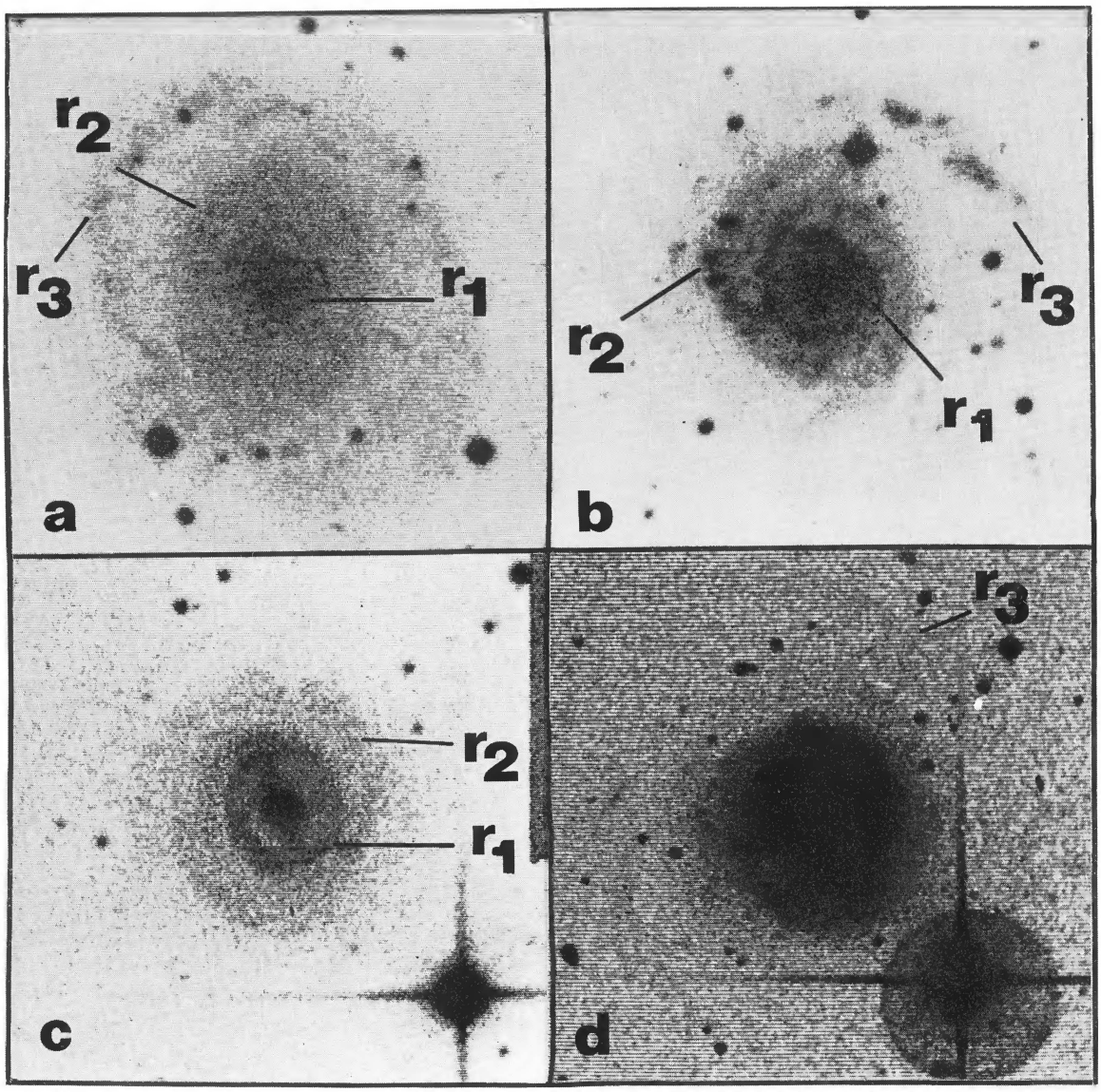

FIG. 9.—Three examples of an SA and one example of an SB galaxy having three distinct ringlike or lenslike zones: (*a*) NGC 6753; (*b*) NGC 7637; (*c*) NGC 3783, to emphasize inner regions; (*d*) NGC 3783, to emphasize very faint outer ring; (*e*) A0227.5−4843, to emphasize very small nuclear (r_1) ring (image from ESO *B*); (*f*) A0227.5−4843, to emphasize inner (r_2) ring/spiral zone; (*g*) A0227.5−4843, to highlight very faint outer (r_3) ring; (*h*) A1035.1−2603. The features of interest are labeled according to a "ring-identification" scheme described in the text.

BUTA (*see* page 616)

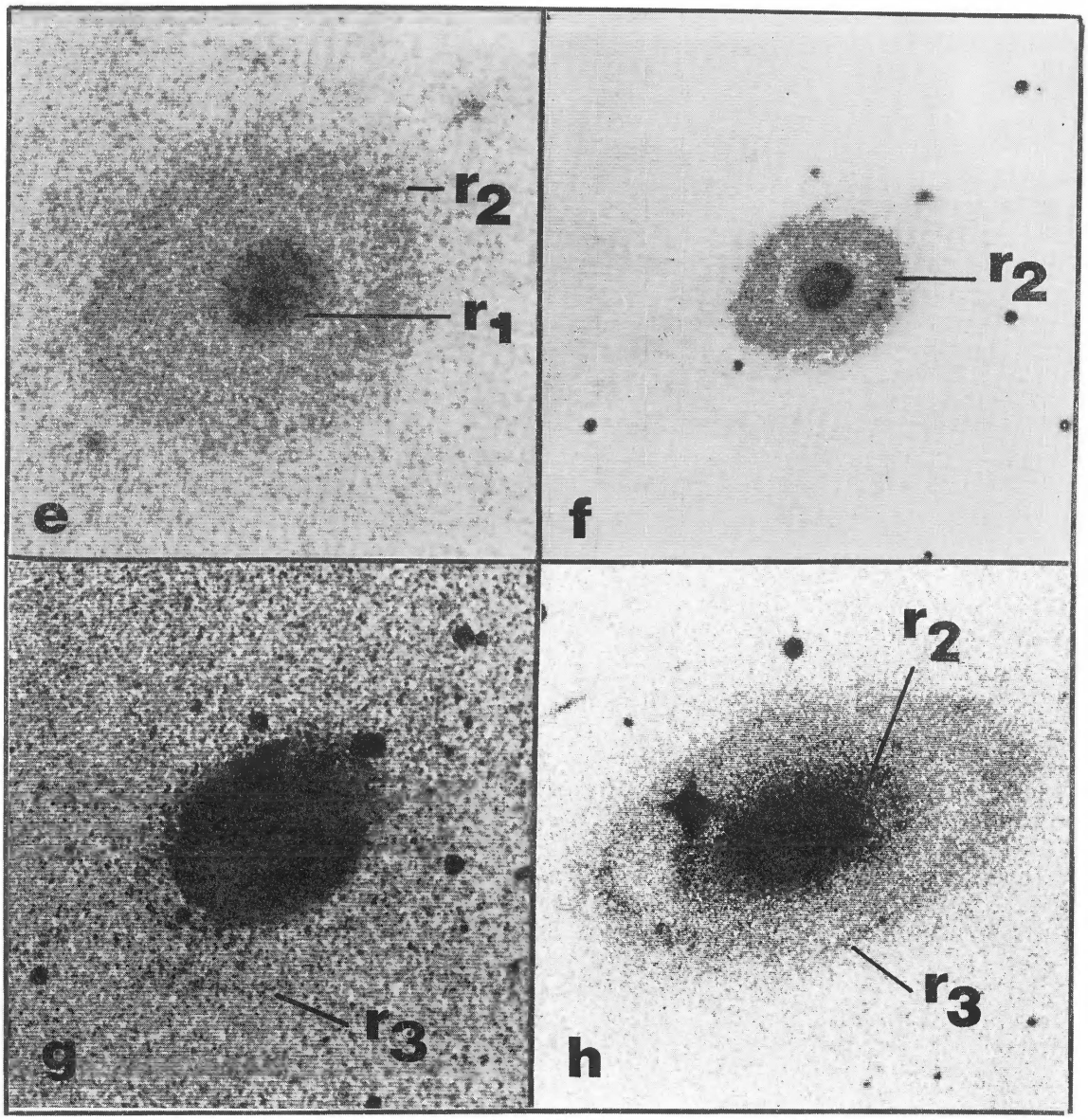

FIG. 9—*Continued*

systems or to nuclear rings in barred systems, r_2 will refer to any analogs of the inner rings of SB systems having a ratio close to 2.0 with respect to an outer ring or pseudoring, while r_3 will refer to all possible types of outer rings or pseudorings. How can a ring be placed in the first, second, or third categories will be discussed in § V*c*. Figure 9 labels the features for the illustrated cases.

Finally, Figure 9*h* shows A1035.1−2603, which shows an outer ring and an intermediate ring; no nuclear ring seems present, however, even on inspection of an ESO *B* chart. Again, the object appears to be nonbarred and yet the rings are quite striking. Other examples of conspicuous rings in what appear to be nonbarred or only very weakly barred galaxies are NGC 3081, NGC 7187, NGC 7531, and NGC 7702 (all to be discussed in future papers in this series) and Hoag's object (O'Connell, Scargle, and Sargent 1974). All of these objects emphasize how strong, obvious bars may not be needed for ring formation. That only mild oval distortions could be just as effective as a typical SB-type bar is highlighted in most recent published calculations of gas response to a barlike potential (Kormendy 1982*a*).

b) Intrinsic Shapes and Orientations

In this section the measurements of the apparent shapes of rings and their relative position angles with respect to bars are used to estimate the intrinsic shapes and orientations of the structures. This is done by comparing the observed distributions with the expected theoretical distributions for a hypothetical sample of randomly oriented infinitesimally thin rings having a variety of intrinsic properties.

i) *Theory*

Using the equations of Stark (1977), it is possible to show (Binggelli 1980) that the apparent axis ratio of a thin elliptical ring having a true axis ratio q_0 and observed with orientation parameters i and ϕ will be

$$q(q_0, i, \phi) = \left(\frac{j + l - \left[(j-l)^2 + 4k^2 \right]^{1/2}}{j + l + \left[(j-l)^2 + 4k^2 \right]^{1/2}} \right)^{1/2}, \quad (1)$$

where

$$j = q_0^2 \sin^2 \phi \cos^2 i + \cos^2 \phi \cos^2 i, \quad (2a)$$

$$l = q_0^2 \cos^2 \phi + \sin^2 \phi, \quad (2b)$$

$$k = (1 - q_0^2) \sin \phi \cos \phi \cos i. \quad (2c)$$

These equations assume that the ellipse is in the equatorial plane of a sphere and is elongated along the x-axis. The inclination, i, is 0° when the ellipse is viewed face-on, and the azimuthal angle, ϕ, increases counterclockwise from the x-axis when $0° \leq i \leq 90°$. The probability distribution for a single value of q_0 is given by

$$F(q_0, q_1, q_2) = 2\pi^{-1} \int_{q_1}^{q_2} \int_0^{\pi/2} \left(\frac{\partial q}{\partial \phi} \right)^{-1} \sin i \, di \, dq, \quad (3)$$

where $q_1 \leq q \leq q_2$ defines the interval of apparent shapes. (Because of symmetry, the integrals are taken only over one quadrant of the sphere.) If the true distribution of shapes is not unimodal, but instead is characterized by a function $f(q_0)$, then the probability distribution is given by

$$F(q_1, q_2) = \int_0^1 f(q_0) F(q_0, q_1, q_2) \, dq_0, \quad (4)$$

The only form of $f(q_0)$ which will be considered here is the following:

$$f(q_0) = 1.0, \quad q_{01} \leq q_0 \leq q_{02}, \quad (5a)$$

$$= 0.0, \quad \text{otherwise}. \quad (5b)$$

It will be justified, at least for SB inner rings, in § V*b*(ii).

If we next assume that this elliptical ring is crossed by a thin, linear bar whose axis coincides with the true major axis of the ring, then the angle between the bar and the apparent major axis of the projected ellipse is

$$\theta_{\text{B,ring}} = \arctan(\cot \phi \cos i) - \frac{1}{2} \arctan\left(\frac{2k}{l-j} \right). \quad (6)$$

If, instead, the ring is crossed by a bar whose axis coincides with the true minor axis of the ring, then the apparent relative position angle is

$$\theta_{\text{B,ring}} = \arctan(-\tan \phi \cos i) - \frac{1}{2} \arctan\left(\frac{2k}{l-j} \right). \quad (7)$$

In each of these equations the first term represents the position angle of the bar, while the second represents that of the apparent major axis of the ring in a coordinate system where $\theta = 0°$ along the line of nodes. These equations can be used to predict the distribution of apparent relative position angles, given by

$$F(q_0, \theta_0, \theta_1, \theta_2) = 2\pi^{-1} \int_{\theta_1}^{\theta_2} \int_0^{\pi/2} \left(\frac{\partial \theta}{\partial \phi} \right)^{-1} \sin i \, di \, d\theta, \quad (8)$$

where θ_0 is the true orientation of the bar in the plane of the galaxy, and $\theta_1 \leq \theta \leq \theta_2$ defines an interval of apparent relative position angles. (Like eq. [3], eq. [8] is for an integration over a quadrant of the sphere, which is all that is required if the bar is aligned or antialigned with the true major axis of the ring. For the case of a bar misaligned with this axis, it would be necessary to integrate over two quadrants.)

Equations (1)–(8) predict very simple expectations. Several distributions are illustrated in Figure 10 for various values of q_0 and of θ_0. For intrinsically round rings ($q_0 = 1.0$), the distribution of apparent axis ratios will be uniform for equal intervals of q, while for elliptical rings ($q_0 < 1$) there will always be a deficiency of apparently round objects and an excess of objects in a bin which includes the preferred shape (Fig. 10*a*). A large dispersion in the values of q_0 has the effect of smoothing out and broadening the excess peak and increasing the frequency of apparently round objects. For

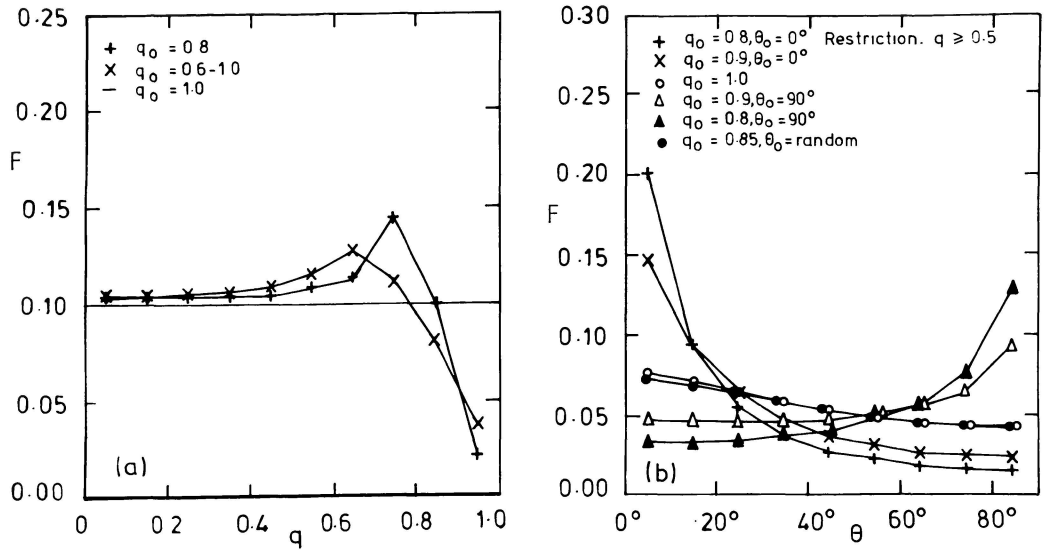

FIG. 10.—Examples of expected relative frequency distributions (see eqs. [1]–[8]) for hypothetical samples of randomly oriented, infinitesimally thin rings having various values of q_0, the intrinsic axis ratio, and θ_0, the intrinsic bar/ring position angle. The curves are in histogram form, but are plotted in the indicated manner for clarity. The frequency F is the fraction of solid angle on a sphere within which a ring having intrinsic parameters q_0 and θ_0 appears in projection to have parameters q and θ in intervals $q_1 \leq q \leq q_2$ and $\theta_1 \leq \theta \leq \theta_2$, respectively.

intrinsically round rings the distribution of apparent relative bar/ring position angles (viewed over a quadrant of the sphere) will be uniform for equal intervals of the parameter

$$A = 2\pi^{-1}\left[\theta + \tfrac{1}{2}\tan\theta \ln(1+\cot^2\theta)\right]. \quad (9)$$

For $0° \leq \theta \leq 90°$, $0 \leq A \leq 1$. However, the serious selection effects for highly inclined galaxies (which would contribute the bulk of objects having low values of θ) would cause an observed distribution to be skewed toward $A = 1$. It is more enlightening in this case to plot an observed distribution, where a serious cutoff in q is usually present, against the angle θ, as in Figure 10*b*. This shows how the distributions for round rings and for elliptical rings where the bar is *randomly* oriented within the ring are only slightly nonuniform, while the distributions for elliptical rings having a preferred alignment with respect to the bar have excess numbers of objects in a bin which includes the preferred angle.

Naturally, these equations will provide only the very simplest model of bars and rings. Real bars are not thin lines, and rings often are not elliptical but can be rectangularly oval, hexagonal, or diamond-shaped. For the purposes of my analysis these complications can be ignored. My procedure will be to compute the expected distributions of apparent shapes or angles, compare them with the observed distributions via a χ^2 analysis, and then adopt the distribution which gives the minimum value of χ^2.

ii) *Observed Distributions*

1. *Inner rings.*—Of the 1200 galaxies in the new sample, 951 were judged to have inner rings or pseudorings. Of these, 478 were classified as SB, 301 as SAB (including SAB and SAB types), and 172 as SA. Since the sample of SA systems is smaller than for SB or SAB systems, I will add the data from Buta (1984*a*) to improve the statistics. I divide the statistics according to family, especially since the SAB category includes a heterogeneous mixture of rings of different types.

Figure 11 illustrates the apparent distributions (*large crosses*). Only inner rings larger than 0.45, the approximate median diameter of all the rings in the sample, have been used. The distributions are also restricted to the range of types $S0^0$ to Sc, and, more important, the parts of the distributions for $q_r \leq 0.40$–0.50 are largely ignored. This is because the distributions for highly inclined galaxies suffer from serious selection effects, since both rings and bars are easily lost when observed at a large inclination angle. A serious deficiency of objects was observed with $q_r < 0.50$ for SB objects, while for SA and SAB objects the selection effect was most severe for $q_r < 0.3$. It is probable that some objects lost to the SB category were included in the SA or SAB categories, hence any conclusions based on the distributions for $q_r < 0.5$ would be in serious error.

Fortunately, as shown in Figure 10*a*, the part of the distributions which gives the most information on intrinsic shapes is that for $q_r \geq 0.50$. In this region the only serious problem would be observational errors, but to minimize the influence of errors the bins have been chosen to have a width of 0.100–0.125, or about twice the mean error in the axis ratios. The distributions are seen to be clearly different for SA and SB galaxies. For SA galaxies the relative frequencies are roughly equal in the range $0.50 \leq q_r \leq 1.00$, while for SB galaxies there is a serious deficiency of apparently round rings. The most promising simulated representations of these apparent distributions are superposed on the data in Figures 11*a* and 11*c*. It was found that unimodal or Gaussian distributions of intrinsic shapes could not reproduce them as well as the simple distributions represented by equations (5). For SA galaxies the data favor intrinsic shapes uniformly spread over a range $q_0 = 0.85$–1.00, while for SB galaxies the range is $q_0 = 0.60$–0.95. Thus SB inner rings on average are more

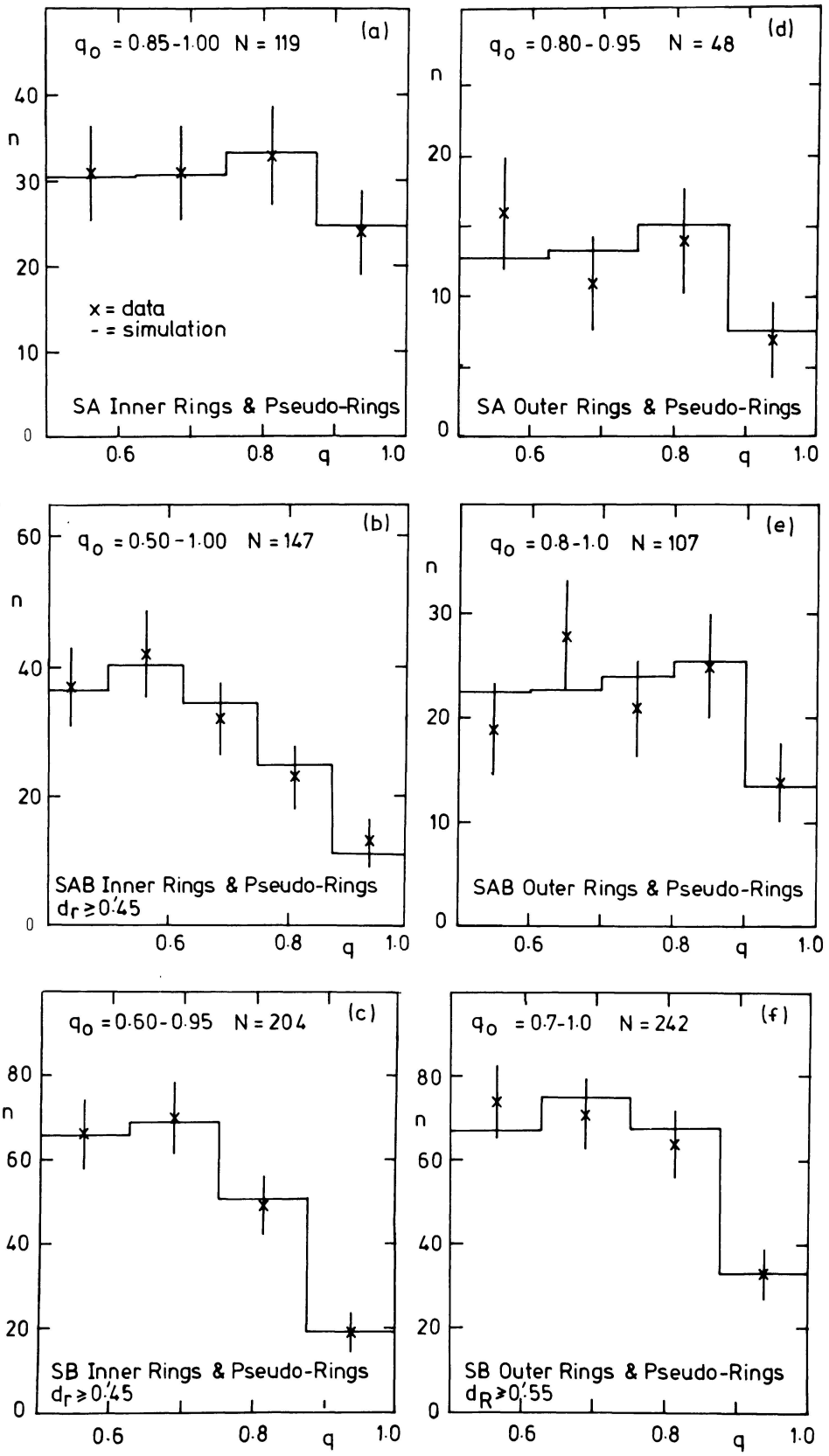

FIG. 11.—Distributions of apparent axis ratios of (*a*) SA inner rings; (*b*) SAB inner rings; (*c*) SB inner rings from the new survey; (*d*) SA outer rings; (*e*) SAB outer rings; and (*f*) SB outer rings. Crosses represent the data, while the solid lines represent simulations (see text) binned in the same manner for a hypothetical sample of thin, planar ellipses having random orientations of the spin axis to the line of sight.

elongated than SA inner rings, a fact already obvious 30 years ago (de Vaucouleurs 1956; de Vaucouleurs and de Vaucouleurs 1964). Note that Buta (1984*a*) and Schwarz (1984*a*) both favored an average intrinsic axis ratio of 0.80 ± 0.05 for SB inner rings, while Kormendy (1979) favored an intrinsic axis ratio of 1.0. A reassessment by Kormendy (1982*a*) is in better agreement with the present results.

The four objects in Figures 6*a*–6*d*, which were chosen to illustrate some variations in the morphology of SB inner rings (§ V*a*[ii]), were also chosen because the shape of the disk suggests that none is highly inclined. Yet note the great differences in the apparent shapes of the inner rings. The outer rings of two of these objects, NGC 6782 (Fig. 6*c*) and A0106.7−3733 (Fig. 6*d*), are also illustrated in Figure 3. Both are seen to have highly elongated inner rings, the axis ratio being 0.63 for NGC 6782 and 0.49 for A0106.7−3733. The disk axis ratios are 0.75 and 0.93, respectively, and note how the outer ring of NGC 6782 is almost orthogonal to the long axis of the inner ring. In contrast to these two, NGC 824 (Fig. 6*a*) and A1307.2−4610 (Fig. 6*b*) show inner rings which appear almost exactly round. In fact, NGC 6782 and A1307.2 −4610 provide a striking contrast because the outer disks are very similar. If we examine only the galaxies where the outer ring or disk axis ratio is 0.85 or greater, assuming that they must be seen close to face-on, we obtain the histogram in Figure 12. (To improve the statistics, data from Buta 1984*a* have been included as well.) This plot suggests that the true distribution may be slightly peaked in the $q_0 = 0.75$–0.88 bin rather than flat over the larger range, which probably explains why both Buta (1984*a*) and Schwarz (1984*a*) deduced a mean axis ratio of about 0.80. Nevertheless, a constant distribution over a range 0.6–1.0 is a reasonable representation, and justifies equations (5) in the first approximation.

Further evidence for a large range in the intrinsic shapes of SB inner rings was inferred by Buta (1984*a*) from kinematics of several selected systems. For example, TAURUS Fabry-Perot interferometer data obtained for the inner ring of NGC 1433 shows that the line of nodes is nearly along an axis perpendicular to the ring, yet the ring appears highly elongated ($q_r = 0.72$). Using a typical value of the rotation velocity to obtain an inclination gives a true axis ratio of $q_{0r} = 0.65 \pm 0.03$. Such a large eccentricity is corroborated by possibly significant noncircular motions found in the ring in spite of the fact that the galaxy is practically face-on (see Paper II). In contrast, the kinematics of a similar barred spiral, NGC 3351, favors a true inner-ring axis ratio of only 0.85–0.90, and little evidence for noncircular motions in the ring is observed.

Although it might be expected that SAB inner rings would be intermediate in properties between SA and SB rings, Figure 11*b* suggests that this is not the case. Instead, the distribution of apparent axis ratios favors a distribution of true ellipticities in the range 0.5–1.0, i.e., slightly more elongated than SB inner rings. The cause of this apparent lack of continuity is the heterogeneous nature of the features I have classified as rings in these systems. As discussed in § V*a*(iii), there exists a class of barlike features which appear strictly in the form of a ring/lens. These features are often highly elongated even in nearly face-on systems, yet no conventional (Saturn or sliver) bar appears to cross them as in typical SB(r)

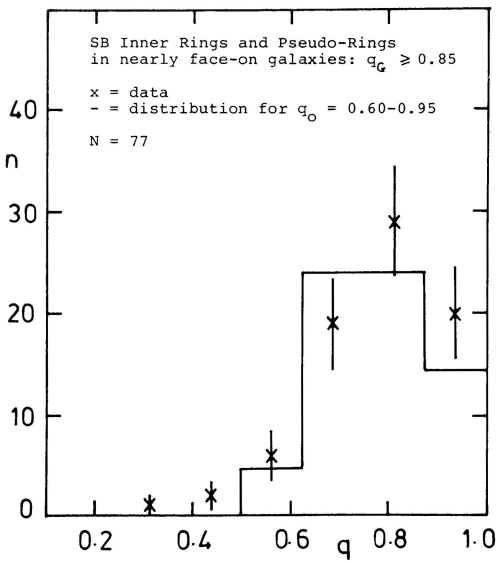

FIG. 12.—Distribution of apparent axis ratios (*crosses*) for a sample of 77 SB inner rings in galaxies where the outer ring has an apparent ridgeline axis ratio $q_R \geq 0.85$, or the outer disk has an isophotal axis ratio $R_{25}^{-1} \geq 0.85$. The sample includes not only data from the new survey, but also independent data from Buta (1984*a*). The distribution is meant to provide a rough idea of what the true distribution of SB axis ratios must be. For comparison the graph shows the expected form of this plot, binned in the same manner, for a distribution of true shapes uniformly spread between $q_0 = 0.60$ and $q_0 = 0.95$ (*solid line*).

systems. It is likely that the ring/lens features contribute the bulk of the most eccentric features, while the other types contribute the less eccentric features. When the former cases are rejected, the preferred range is $q_0 = 0.7$–1.0.

Given that SB and SAB inner rings are on average elongated, we next ask whether these structures have any preferred orientations with respect to bars. Figure 13 compares the apparent distributions of relative position angles with the simulated distributions expected for a sample of randomly oriented ellipses. To allow for the selection effects for $q_r < 0.50$, the simulations and the observed distributions have been restricted to $q_r \geq 0.50$. Figures 13*a* and 13*b* show that both SB and SAB inner rings prefer low angles with respect to the bar in projection. The distributions are well represented by simulations where the inner rings are intrinsically oriented parallel to the bar (compare with Fig. 11*b*). Very few inner rings must be oriented perpendicular to bars, because this would give rise to an excess of objects having large apparent angles with respect to the bar. Random orientations also appear to be ruled out, because this would give rise to an almost uniform distribution with θ.

2. *Outer rings.*—The new survey produced a sample of 578 outer rings and pseudorings for this analysis. Of these, 379 occurred in galaxies classified as SB, 126 in galaxies classified as SAB, and 63 in objects classified as SA. It is clear that outer rings are less frequently detected than inner rings, probably because the surface brightness on average is lower than for inner rings. Figures 11*d*–11*f* illustrate the distributions of apparent axis ratios (*crosses*), separated according to family. Here selection effects again were found to be

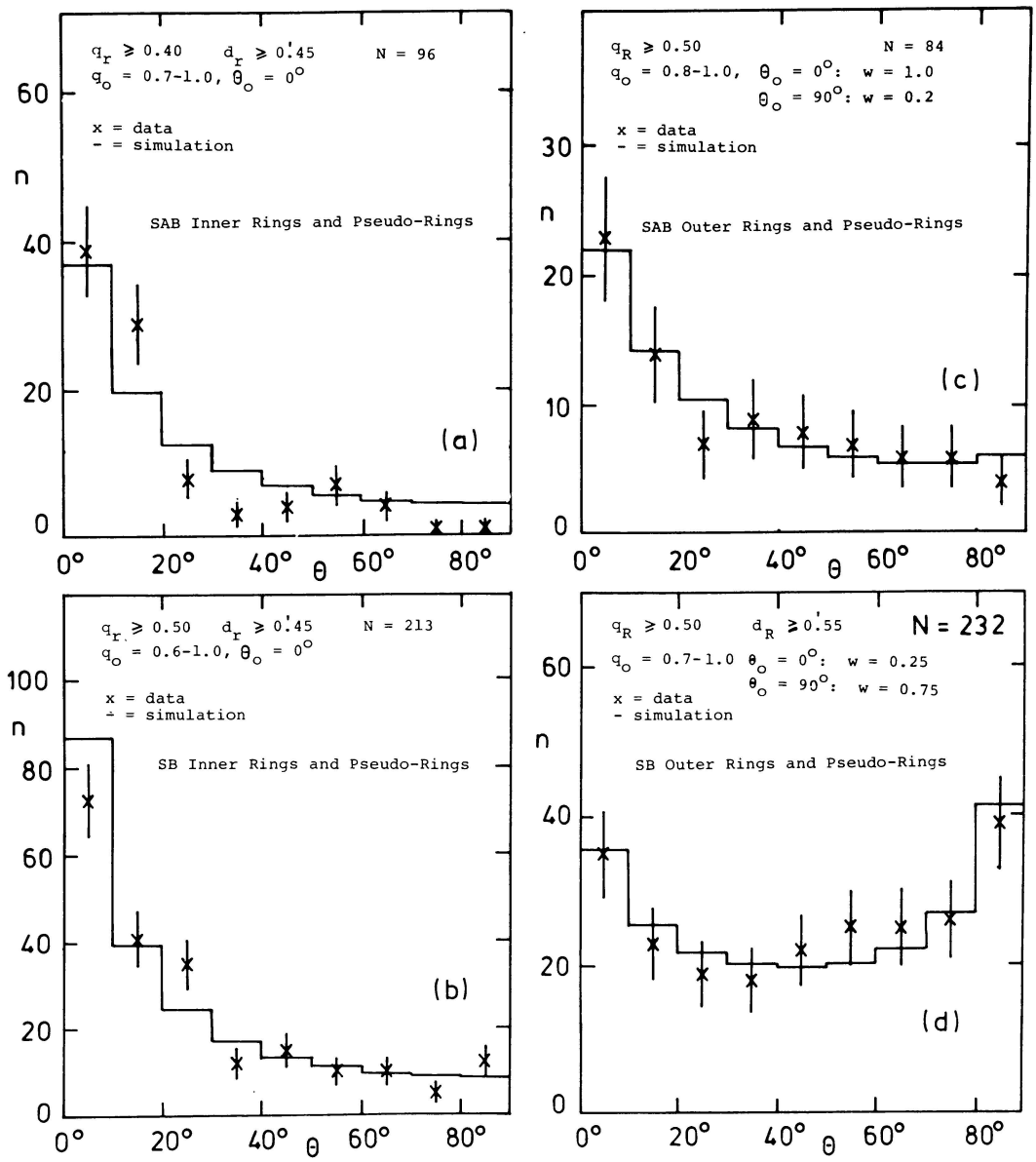

FIG. 13.—Distributions of apparent relative angles for (*a*) SAB inner rings; (*b*) SB inner rings; (*c*) SAB outer rings; and (*d*) SB outer rings. For comparison, simulations of the distributions expected for samples of randomly oriented ellipses where the ring has preferred alignments (either parallel or perpendicular) with respect to the bar are superposed on the data. Note how representations where the bar is intrinsically oriented parallel to the ring are good for inner rings and SAB outer rings, while SB outer rings require two preferred alignments, parallel and perpendicular, to the bar.

important for $q_R < 0.5$, so the statistics are restricted as for inner rings to $q_R \geq 0.5$. The distribution was found to be peculiar for SA outer rings, in the sense that the relative frequencies increased steadily to $q_R = 0.40$, and then the selection effect appeared to set in. As for inner rings, there could be a tendency to misclassify some barred systems as nonbarred when the inclination is high, so the statistics must be unreliable for $q_R < 0.50$. Also, for these SA objects the survey produced only a very small sample, hence Figure 11*d* includes all the SA outer rings from Buta (1984*a*) in addition to the new survey objects.

The best simulated representations of these outer ring distributions are superposed on the data in Figure 11. As for inner rings, the distributions favor different ranges of intrinsic shapes for each family. For SA outer rings, the favored range is $q_0 = 0.80$–0.95, while for SB outer rings the favored range is 0.7–1.0. Thus, SB outer rings on average are more elongated intrinsically than SA outer rings but nevertheless are less eccentric on average than SB inner rings. For SAB outer rings the favored range is $q_0 = 0.8$–1.0, also less eccentric than SAB inner rings. Note that for the simulations I have again assumed that the distribution of true ellipticities is represented by equations (5). This is uncertain for outer rings, and one may well question whether the possibility that some have $q_0 = 0.7$ is an artifact of this simple model. The average axis ratio, 0.85–0.90, is, however, certainly plausible.

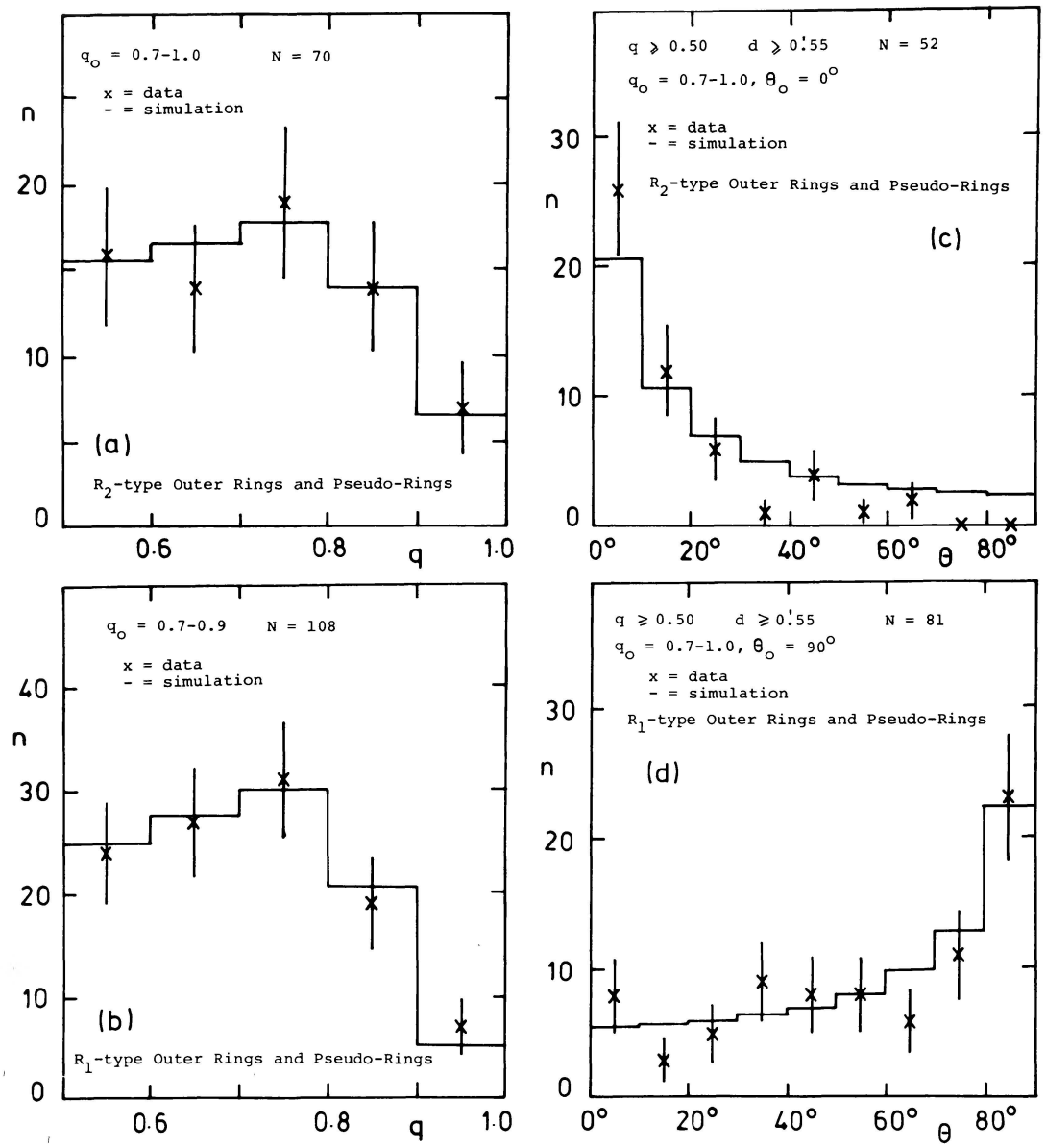

FIG. 14.—Distributions of apparent axis ratios for outer rings and pseudorings classified as being of (*a*) R_2 type and (*b*) R_1 type. These plots demonstrate that R_1 rings may be more eccentric on average than R_2 rings, but the difference is only barely significant. For the same ring types, panels *c* and *d* show the distributions of relative bar/ring position angles. Note how R_2-type rings prefer low angles with respect to the bar, while R_1-type rings prefer large angles.

In § V*a*(i) it was argued that some outer rings show the form expected for theoretically simulated rings which develop near the OLR in particle dynamical models. In Figures 14*a* and 14*b* the distributions for outer rings classified as R_2 or R_1 are compared with the best-fitting simulations. These apparent distributions include the dominant component in dual-mode cases [those having the $(R_1'R_2')$ characteristic]. Figure 14 shows that there is some indication that R_1-type outer rings on average are more elongated intrinsically than R_2-type outer rings, though the difference cannot be established at a high significance level with the present data. The difference, if real, could be interpreted as being due to the larger average radius of the OLR^+ orbits compared with the OLR^- orbits, and the consequently weaker influence of the bar.

Given that outer rings on average are eccentric, we now ask whether they have any preferred orientation with respect to bars. Figures 13*c* and 13*d* illustrate the distributions of apparent relative position angles for SB and SAB outer rings, and demonstrate a striking difference with inner rings. The distribution of angles for SB outer rings shows *two* peaks, one at small angles with respect to the bar and one at large angles with respect to the bar. Figure 13*d* shows that this distribution is well represented by two intrinsic modes of preferred alignment: a dominant perpendicular mode and a second parallel mode. In contrast, Figure 13*c* shows that SAB outer

rings and pseudorings almost exclusively favor parallel alignment, just as for inner rings. However, I believe that the two modes are nevertheless presented in SAB systems (there are numerous unambiguous cases), and that these statistics simply imply that the parallel mode is more dominant than the perpendicular mode for these objects.

The existence of two preferred alignments for outer rings provides strong support for a link between these structures and the outer Lindblad resonance. In Figures 14*c* and 14*d* this link is made firmer by restricting the statistics to SAB and SB outer rings classified as being of R_1 or R_2 type. These comprise 55% of the objects in Figure 13*d*. Figure 14 shows that R_2-type outer rings are usually observed at low angles with respect to the bar in projection, while R_1-type rings are observed at larger angles. Comparison with simulated distributions shows that the R_2 distribution is well represented with an intrinsic orientation parallel to the bar, while the R_1 distribution favors an intrinsic orientation perpendicular to the bar.

The conclusions arrived at from Figures 11–14 are not consistent with previous work. Kormendy (1979), Buta (1984*a*), and Schwarz (1984*a*) all concluded that outer rings are preferentially aligned perpendicular to bars with an average intrinsic axis ratio of about 0.9. There are two possible reasons for this oversight. One is that the parallel mode is simply less frequent than the perpendicular mode and hence would be easily missed in small samples. The simulation in Figure 13*d* required that the relative frequency of the perpendicular mode be 3 times that of the parallel one, although if SAB outer rings are taken into account the two modes may be almost equally frequent. The second reason is a selection effect, probably due to surface brightness, which was overcome by the depth and high quality of the J survey charts.

3. *r_1 rings.*—Section V*a*(vi) brought attention to a class of objects where three rings or pseudorings can be identified in the light distribution. The smallest of these rings, the r_1 rings, are often classified as inner rings, yet they are analogs more of the nuclear rings in conventional barred spirals than of the inner rings of those objects. The new survey, together with the data provided by Buta (1984*a*), allows us to assess more carefully some of the intrinsic properties of these small ring structures. Note that in Figure 11*a*, the distribution favors r_2 rings since these are often observed in SA systems as well (see, for example, Figures 9*e*–9*g*).

Figure 15 illustrates the distribution of apparent axis ratios for (*a*) nuclear and r_1 rings in SB and SAB spirals and (*b*) r_1 rings in SA spirals. In spite of the small sizes of the samples, the distributions appear to be similar. The numbers of objects in both cases were found to drop off for $q < 0.5$, presumably because of recognition difficulties. Both distributions are well represented by a simulation where $q_0 = 1.0$, although a range of true axis ratios (say from 0.9 to 1.0) is not ruled out at a high significance level. It appears that r_1 rings on average may be rounder than inner or even outer rings, a fact which may be due to the stronger influence of the spheroid on the orbits in the inner regions. This seems to be true even for barred or weakly barred systems where the bar lies inside r_1, although I suspect that for the nuclear rings of barred systems where the bar fills r_2 instead, there may be a larger range of true

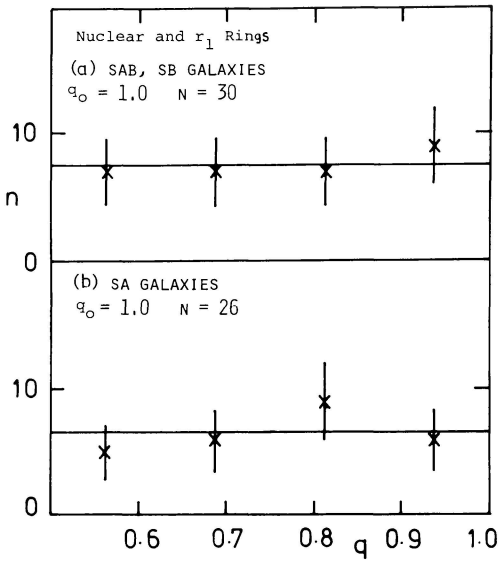

FIG. 15.—Distributions of apparent axis ratios for (*a*) nuclear rings and r_1 rings in SAB and SB galaxies; (*b*) r_1 rings in SA galaxies. The samples include data not only from the new survey but also from Buta (1984*a*). Both distributions are well represented by simulations where $q_0 = 1.0$, indicating that these small rings are rounder on average than inner or outer rings.

eccentricities (Buta 1984*a*). This is highlighted by NGC 1317 and NGC 1433, where the nuclear rings are significantly oval even though the galaxies are very little inclined.

Note that the analogy between nuclear rings and r_1 rings is something that remains to be more firmly established. It may be possible to do this using detailed rotation curve data (Buta 1984*a*).

4. *Test for preferred alignments using (R)SB(r) or (R_1R_2)SB galaxies.*—Since SB and SAB galaxies occasionally have both inner and outer rings, and some even have two outer rings, another way of searching for preferred alignments would be to compare the position angles of the two features relative to the bar. This approach has an advantage over simple angle distributions in that the two rings are observed with the same orientation parameters. It was first used by Buta (1984*a*) on a sample of 20 (R)SB(r) objects, and I extend that analysis to the much larger sample of data provided by the new survey.

Figures 16*a* and 16*b* show graphs of the apparent relative position angle between the major axes of the inner and outer rings, θ_{rR} plotted against the apparent angle between the bar and the inner ring, θ_{Br}, for samples of 206 SB and 57 SAB galaxies, respectively. If inner and outer rings have the same alignment with respect to the bar, or are both round, then the points in this kind of plot should scatter near $\theta_{rR} = 0°$ (note that only angles between 0° and 90° are considered). However, both plots show that points more or less fill the entire zone to the left of the diagonal of the square area. The effect is more pronounced for SB than for SAB systems. To test what the observed distribution of the points means, Figure 17 shows two simulations where (*a*) the (r) is parallel to the bar while the (R) is perpendicular to the bar, and (*b*) the (R) is parallel to the bar while the (r) is perpendicular to the bar. The assumed intrinsic axis ratios are 0.80 for the inner ring

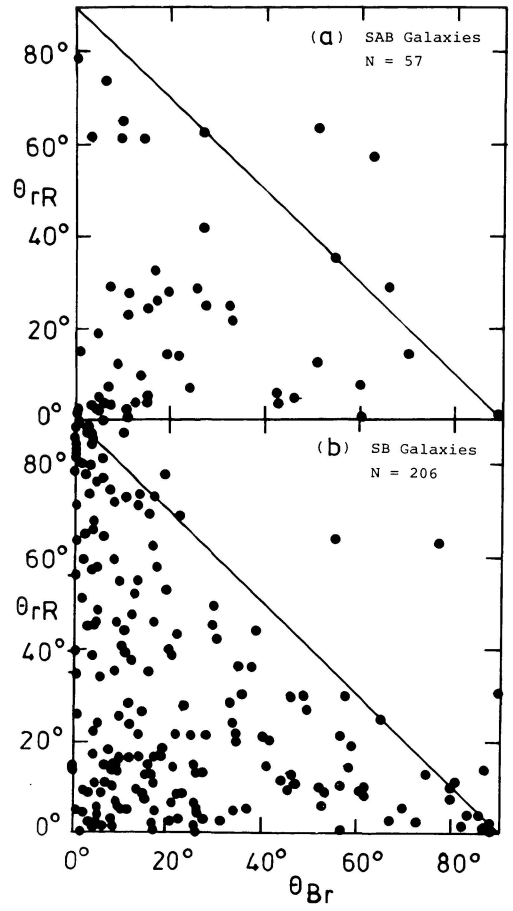

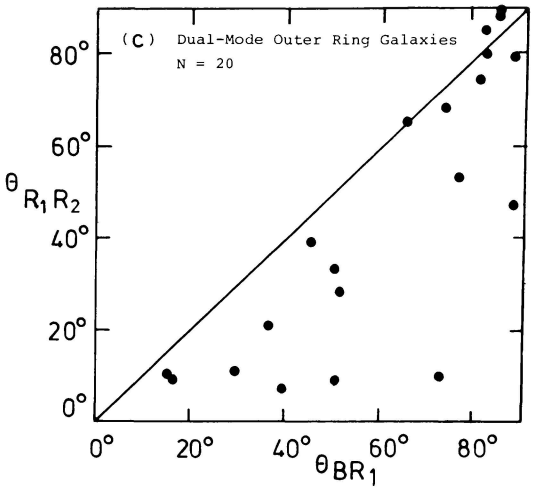

FIG. 16.—This plot compares the relative position angle between the major axes of the inner and outer rings in (*a*) double-ring SAB galaxies and (*b*) double-ring SB galaxies, with the angle between the bar and the inner ring. Note how points in each case mainly fill only the region to the left of the diagonal. In panel *c* the same kind of plot is made for the relative angle of the two outer rings in systems having the ($R'_1R'_2$) characteristic. Note how the points in this case fill only the right half of the diagram.

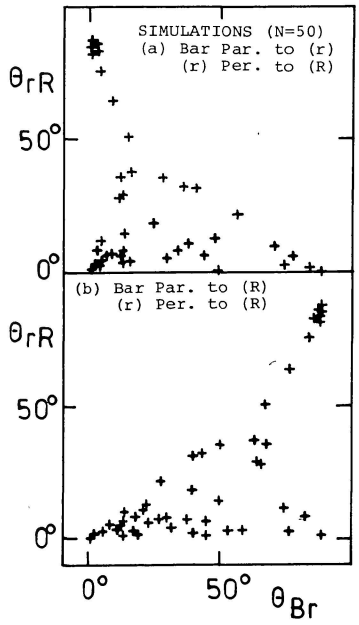

FIG. 17.—Simulations of the expected distributions of points in the (θ_{rR}, θ_{Br})-plane for (*a*) a case where the inner ring is aligned along the bar with an axis ratio of $q_0 = 0.80$, while the outer ring is aligned perpendicular to the bar with an axis ratio $q_0 = 0.90$, and (*b*) the alternate case where the rings are still perpendicular but the bar is aligned along the outer ring. These simulations demonstrate that the preference of points to the left of the diagonal in Figs. 16*a* and 16*b* can be explained if a significant fraction of the objects have an inner ring aligned parallel to the bar and an outer ring perpendicular to the bar. The preference of points to the right of the diagonal in Fig. 16*c* can be explained if R_1 outer rings and pseudorings are aligned perpendicular to bars while R_2 outer rings and pseudorings are aligned parallel to bars.

and 0.90 for the outer ring. Figure 17*a* shows that the form of the distribution of points in Figure 16 can be explained if a significant fraction of the objects has an inner ring in parallel alignment and an outer ring in perpendicular alignment. The case for this is fairly strong, because if the alternate orientations were instead true, the points should occupy the right half of the (θ_{Br}, θ_{rR})-plane (Fig. 17*b*). If the bar were randomly oriented with respect to the rings, points would be expected to occupy the full square area. Double-ring SB galaxies support the notion that many inner and outer rings have preferred, perpendicular alignments with the bar parallel to the (r). Note that Figure 16 does not distinguish the two modes of outer ring, because in two-ring systems with a parallel-mode outer ring, the points will scatter near $\theta_{rR} = 0°$. The two modes would be manifested in a larger than expected frequency of objects having low values of θ_{rR}.

As a final application of this approach, Figure 16*c* shows a graph of the relative position angle between the long axes of

TABLE 1

RESULTS OF χ^2 FITS

Sample (1)	N (2)	q_0 (3)	θ_0 (4)	Frequency (5)	χ^2 (6)	ν (7)	Probability (8)	Notes (9)
A. Inner Rings								
SA axis ratios	119	0.85–1.00	...	...	0.04	2	98%	
SAB axis ratios	147	0.50–1.00	...	...	0.68	3	71	
SB axis ratios	204	0.60–0.95	...	...	0.07	2	97	
SAB angles	96	0.70–1.00	0°	1.00	16.94	6	1	1
SB angles	213	0.60–1.00	0	1.00	11.94	6	6	1
B. Outer Rings								
SA axis ratios	48	0.80–0.95	...	...	1.34	2	50	
SAB axis ratios	107	0.80–1.00	...	...	2.18	3	53	
SB axis ratios	242	0.70–1.00	...	...	1.13	2	58	
R_2, R'_2 axis ratios	70	0.70–1.00	...	...	0.51	3	92	
R_1, R'_1 axis ratios	108	0.70–0.90	...	...	0.82	3	85	
SAB angles	84	0.80–1.00	0°	0.83	2.49	3	48	
		0.80–1.00	90	0.17	...	...	...	
SB angles	232	0.70–1.00	0	0.25	2.76	3	43	
		0.70–1.00	90	0.75	...	...	...	
R_2, R'_2 angles	52	0.70–1.00	0	1.00	11.61	6	7	
R_1, R'_1 angles	81	0.70–0.90	90	1.00	5.38	6	49	
C. Nuclear and r_1 Rings								
SA axis ratios	26	1.00	...	...	0.40	2	86	2
SAB, SB axis ratios	30	1.00	...	...	1.37	2	50	3

Col. (1).—Samples of rings used in statistics, divided either by family or according to the form of the outer ring (see text).

Col. (2).—Number of objects in sample for fit.

Col. (3).—Range of intrinsic axis ratios required to reproduce the observed apparent distribution of axis ratios.

Col. (4).—Preferred intrinsic alignment angle between the bar and a given ring type required to reproduce the observed apparent distribution of projected relative position angles.

Col. (5).—Assumed relative frequency of alignment mode.

Col. (6).—Value of χ^2 derived from best fitting simulated distribution for a sample of thin elliptical rings randomly oriented to the line of sight (observational error is not explicitly taken into account, but parts of the apparent distributions affected by selection effects are excluded from the comparisons).

Col. (6).—Number of degrees of freedom in comparison.

Col. (7).—Probability that departures of the observed distribution from the simulated distribution are due to random sampling errors.

NOTES.—(1) These simulations assume perfect parallel alignment, but some cases may be in serious misalignment. (2) Sample includes r_1 rings from Buta 1984*a*. (3) Sample includes nuclear rings in SAB and SB systems from Buta 1984*a*.

the outer rings in dual-mode systems, $\theta_{R_1R_2}$, plotted against the angle between the bar and the innermost ring, θ_{BR_1}. The resulting distribution of points is similar to Figure 17*b*, and suggests that the two structures are intrinsically perpendicular to each other.

5. *Summary of results.*—The results of the large number of comparisons made in the previous sections are summarized in Table 1. Except for the angle distributions, the χ^2 fits indicate that the simulated distributions are excellent representations of the observed distributions over the indicated ranges of apparent axis ratios. The comparisons are poorer but still very acceptable for the angles. The poorer agreement for the angles is due in part to the difficulty of measuring precise relative bar/ring position angles for these small objects, and in part to the simplicity of the model (thin linear bar). Some bars are oval and fairly fat, and in projection would yield an angle different from that expected for a linear bar.

c) *Ring Ratios*

The final property of ringed systems that I consider is the ratios of ring radii in those objects having two or more rings.

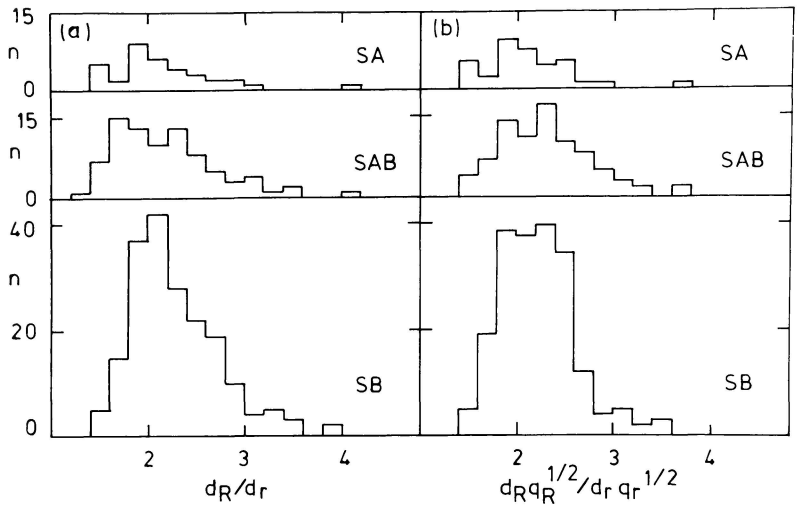

FIG. 18.—(*a*) Distributions of the apparent ring major-axis diameter ratio d_R/d_r, separated according to family, based on data from the new survey; (*b*) same samples as in panel *a*, except that the ratio of geometric mean diameters is used.

TABLE 2

MAJOR-AXIS AND GEOMETRIC MEAN RING DIAMETER RATIOS VERSUS FAMILY

	MAJOR-AXIS DIAMETER RATIO			GEOMETRIC MEAN DIAMETER RATIO			
FAMILY (1)	$\langle d_R/d_r \rangle$ (2)	σ (3)	N (4)	$\langle d_R q_R^{1/2}/d_r q_r^{1/2} \rangle$ (5)	σ (6)	N (7)	NOTES (8)
SA	2.08 ±0.07	0.43	34	2.07 ±0.06	0.36	34	
	2.05 ±0.07	0.40	33	2.05 ±0.06	0.34	33	1
SAB	2.18 ±0.06	0.54	83	2.29 ±0.05	0.47	83	
	2.11 ±0.05	0.45	79	2.25 ±0.05	0.41	80	1
SB.....	2.29 ±0.04	0.51	198	2.24 ±0.03	0.44	198	
	2.23 ±0.03	0.40	190	2.19 ±0.02	0.34	191	1

Col. (1).—Family of sample (type range $S0^0$ to Sc).

Col. (2).—Mean value of the ratio of the major-axis diameters of outer and inner rings in double-ring systems; in some systems with three rings or pseudorings, the ratio is $d(r_3)/d(r_2)$.

Col. (3).—Standard deviation about the mean.

Col. (4).—Number of objects in sample.

Col. (5).—Mean value of the ratio of the geometric mean diameters of outer and inner rings.

Col. (6).—Standard deviation about the mean.

Col. (7)—Number of objects in sample.

NOTE.—(1) After one cycle of 2 σ rejection.

Kormendy (1979) and Athanassoula *et al.* (1982) showed that in double-ring SB galaxies, the ratio d_R/d_r is approximately equal to 2, consistent with a hypothesis that the inner rings are close to CR and the outer rings are associated with the OLR. Buta (1984*a*) showed that a similar ratio was observed for $d(r_3)/d(r_2)$ in double-ring SA galaxies as well, suggesting that the same resonances are involved, but that when nuclear rings or their analogs could be unambiguously identified, the ratio was usually much larger than 2. With the present large data set, we can examine the ratios in more detail than could be done before.

Figure 18*a* shows the distributions of major-axis ring diameter ratios for 198 SB, 83 SAB, and 34 SA systems. In the latter two families, some of the objects are of the "three-ring or pseudoring" type (§ V*a*[vi]). In these cases the ratio is $d(r_3)/d(r_3)$. In agreement with Buta (1984*a*), the ratios are similar in the mean (Table 2) and cover the same range for all three families, hence bar strength is not a major determinant

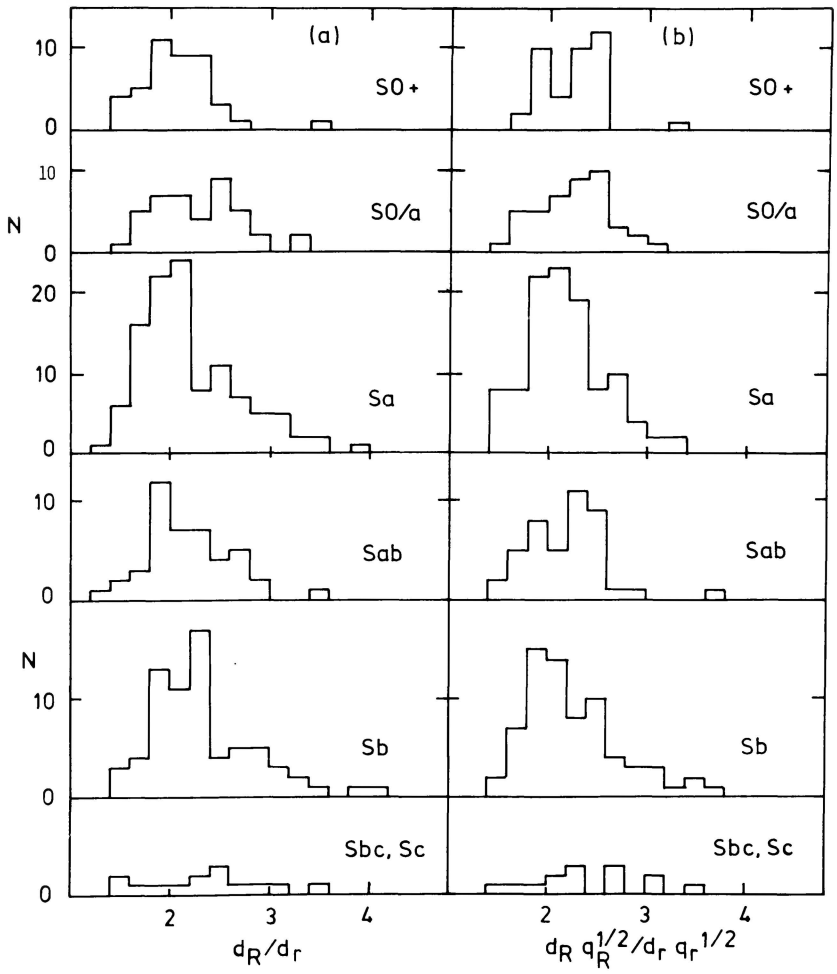

FIG. 19.—(*a*) Distributions of the apparent ring ratio d_R/d_r, separated according to Hubble stage, based on data from the new survey; (*b*) same samples as in panel *a*, except that the ratio of the geometric mean diameters is used.

of the values of these ratios. The spread of the ratios is, however, much larger than would be expected from observational error, and the distributions for all three families are obviously slightly skewed. How much of this could be due to projection effects on elliptical rings having a wide range of true eccentricities and orthogonal alignments?

Figure 18*b* shows that the skewness may be due in part to projection effects. It plots the distributions of the ratios of the *geometric* mean diameters, $d_R q_R^{1/2}/d_r q_r^{1/2}$. Mean values of this ratio are also compiled in Table 2. The skewness is obviously reduced in this representation, but the dispersion is only slightly reduced.

Figure 19*a* shows the dependence of the ratio on Hubble stage after combining all three families (see also Table 3). This demonstrates that the ratio is almost independent of Hubble type in the range S0 to Sc, but that there is nevertheless a slight increase with advancing stage. This is because, as the stage advances, the relative number of objects having $d_R/d_r > 3.0$ increases and leads to a slight increase in the means. Note especially the very skewed character of the distributions for Sa and Sb systems. Again, use of geometric means tends to reduce this skewness (Fig. 19*b*), as well as to reduce the dispersions slightly.

Figure 20 shows histograms of the distribution of ring ratios for the hierarchy $d(r_3)/d(r_2)$, $d(r_3)/d(r_1)$, and $d(r_2)/d(r_1)$. These plots include, in addition to the new sample, the data from Buta (1984*a*). They show that $d(r_3)/d(r_2)$ is strongly peaked near a ratio of 2 with very few larger than 2.5, while the ratio $d(r_3)/d(r_1)$ is very broad and the values are all larger than 2.5. (The range of the latter ratio is certainly affected significantly by selection effects, because the intrinsically smallest r_1 rings would not be detected in a survey based purely on the SRC J or ESO *B* films.) Some two-ring systems also have large ring ratios. Is it possible that in some galaxies, rings of types r_1 and r_3 have formed but not type r_2? Many galaxies have only a single ring, but only in the double or triple ring systems can we make some definitive judgements about the nature of the rings, for example, via ring ratios. Whether only one ring is present or several, it is likely that they are all part of the same hierarchy. The combinations $r_1r_2r_3$, r_1r_2, r_1r_3, r_2r_3, or r_1, r_2, or r_3 alone, certainly appear to exist.

TABLE 3

MAJOR-AXIS AND GEOMETRIC MEAN RING DIAMETER RATIOS VERSUS STAGE

HUBBLE STAGE (1)	MAJOR-AXIS DIAMETER RATIO $\langle d_R/d_r \rangle$ (2)	σ (3)	N (4)	GEOMETRIC MEAN DIAMETER RATIO $\langle d_R q_R^{1/2}/d_r q_r^{1/2} \rangle$ (5)	σ (6)	N (7)	NOTES (8)
S0$^+$	2.07	0.36	39	2.23	0.33	39	
	$\pm$0.06			$\pm$0.05			
	2.04	0.29	38	2.20	0.27	38	1
	$\pm$0.05			$\pm$0.04			
S0/a	2.26	0.43	43	2.25	0.36	43	
	$\pm$0.07			$\pm$0.05			
	2.21	0.38	41	2.25	0.32	41	1
	$\pm$0.06			$\pm$0.05			
Sa	2.23	0.59	107	2.21	0.48	107	
	$\pm$0.06			$\pm$0.05			
	2.16	0.46	103	2.16	0.38	104	1
	$\pm$0.05			$\pm$0.04			
Sab	2.19	0.43	42	2.20	0.39	42	
	$\pm$0.07			$\pm$0.06			
	2.16	0.38	41	2.17	0.33	41	1
	$\pm$0.06			$\pm$0.05			
Sb	2.34	0.53	70	2.27	0.49	70	
	$\pm$0.06			$\pm$0.06			
	2.28	0.44	67	2.19	0.39	66	1
	$\pm$0.05			$\pm$0.05			
Sbc,Sc ...	2.37	0.58	14	2.43	0.54	14	
	$\pm$0.15			$\pm$0.14			

Col. (1).—Revised Hubble stage of sample (families SA, SAB, SB inclusive).

Col. (2).—Mean value of the ratio of the major-axis diameters of outer and inner rings in double-ring systems; in some objects with three rings or pseudorings, the ratio is $d(r_3)/d(r_2)$.

Col. (3).—Standard deviation about the mean.

Col. (4).—Number of objects in sample.

Col. (5).—Mean value of the ratio of the geometric mean diameters of outer and inner rings.

Col. (6).—Standard deviation about the mean.

Col. (7).—Number of objects in sample.

NOTE.—(1) After one cycle of 2 σ rejection.

It is important to reemphasize that bars can exist inside either r_1 or r_2 rings. In the context of resonances, r_1 rings may be related to the ILR because the wide range of values of the ring ratio, $d(r_3)/d(r_1)$, can be explained by the large differences in the shape of the rotation curve known to exist in the inner regions of galaxies. Adding to the spread is the possibility that some galaxies have two ILRs, which could be widely separated if the bulge is weak, and that a ring could then form at either the IILR or the OILR, depending on as yet unknown conditions. The point is that, given the bar and ring hierarchy, it is clear that all SB inner rings might not be associated with an ultraharmonic resonance near CR. Some could be related to ILR.

VI. CONCLUSIONS

The purpose of this paper has been to test the "resonance hypothesis" of galaxy rings by examining their detailed morphology and obtaining statistics of their apparent shapes, relative sizes, and apparent orientations with respect to bars. A major new survey designed for this purpose was described, and subsets of the first 1200 objects measured in the survey were used to deduce the intrinsic shapes and orientations of the structures. The results have strengthened previous indications that inner and outer rings have a fairly wide range of true eccentricities and also have preferred alignments with respect to bars. On average, SA inner and outer rings are rounder than SB or SAB inner and outer rings, while outer rings in general tend to be less eccentric than inner rings. From an analysis of the distributions of apparent relative bar/ring position angles of a large number of objects, it has been found that inner rings almost exclusively are aligned parallel to bars, while outer rings have two preferred alignments: parallel and perpendicular. The two distinct morphologies expected for OLR–type pseudorings were shown to be present in abundance among real outer rings, and furthermore were demonstrated to have orthogonal preferred alignments. An interesting observation is that some galaxies

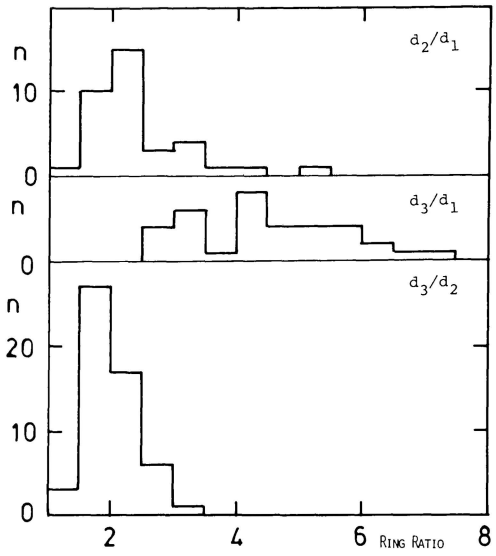

FIG. 20.—Distributions of the apparent ratios $d(r_3)/d(r_2)$, $d(r_3)/d(r_1)$, and $d(r_2)/d(r_1)$ for the rings of "three-ring" systems as defined in the text.

appear to show aspects of both morphologies, implying that both the major families at the OLR could be significantly populated. The morphology of inner rings was also shown to be varied. These occasionally show breaks near the minor-axis points of the bar and can have pointed oval, rectangular, or even slightly hexagonal shapes. They are usually unambiguously distinguishable from outer rings.

A detailed analysis of ratios of ring radii in galaxies of all types and families has confirmed the results of Kormendy (1979) and Athanassoula *et al.* (1982) that outer rings are on average about 2.2 times as large as inner rings in double-ring SB galaxies. The same ratio is found for SA and SAB galaxies where inner rings can be unambiguously distinguished from nuclear or r_1 rings, implying that the same resonances are probably involved. In SA galaxies the r_2 ring is often the boundary of an "intermediate zone" which is lenslike or ringlike. The features usually classified as inner rings in such galaxies are really more analogous to the nuclear rings of SB galaxies.

The observations described here provide strong support for the resonance hypothesis of the origin of rings in most galaxies. Outer rings are now fairly unambiguously identifiable with the outer Lindblad resonance, and hence may be useful in the future to deduce pattern speeds. Inner rings as classified in RC1 probably consist of a mixture of features linked with either the inner Lindblad resonance or the inner second harmonic resonance, the latter being likely for most SB inner rings and the former being likely for SB nuclear rings and some SA inner rings. The SA class also must include some rings near CR, because of the similarity of ring ratios observed for double-ring SA galaxies to those observed for double-ring SB galaxies. Because of the ambiguity and their more eccentric shapes, inner rings may be less useful for measuring pattern speeds than outer rings (but see Paper II).

In spite of this good agreement with the theory, resonances may not be the only way to make rings in galaxies. Some rings may be transient structures, for example, which have developed in response to retrograde tidal encounters (P. J. Quinn, 1983 private communication), while others could represent axisymmetric density waves (Miller 1978). Such features could contribute to the inhomogeneity of the size and shape distributions of rings. Also, in Paper III it will be shown that the bright inner ring in the SA spiral NGC 7531 is located exactly at the turnover radius, and hence the feature may be resulting from some peculiar effect associated with this radius rather than from some specific resonance. Further work will therefore be required to examine other possible formation mechanisms for rings.

One problem with the resonance theory is that the models used for the basis of the present work are purely gasdynamical, yet, as will be shown in the successive papers of this series, most rings are largely stellar. Elmegreen and Elmegreen (1985) have argued that the predominance of stellar spirals in SB galaxies supports theories where the bar is a nonstatic entity, i.e., is growing with time. Therefore, while the present statistics support the predictions of the gasdynamical models of Schwarz, more realistic models may require a nonstatic bar. Finally, it is a little-appreciated fact that the brightest rings in terms of surface brightness and visual strength of the enhancement are observed in nonbarred or very weakly barred galaxies. One of the main requirements for making rings in the Schwarz models is that the nonaxisymmetric forcing be strong enough to make orbits cross in the vicinity of resonances, so that very weak bars should be less effective in inducing this crossing. Yet very bright rings are observed in galaxies which appear to have no bar. Even more enigmatic are nonbarred, ringed S0 galaxies such as NGC 7702, which are very difficult to understand in the context of these models, since they suggest that there may be a mechanism whereby *purely* stellar rings can form in the absence of obvious bars. These problems and others will be addressed in the future papers of this series.

I would like to thank Professor G. de Vaucouleurs for his encouragement and support of this work, Dr. S. M. Simkin for inspiring my early interest in rings, Dr. M. P. Schwarz for allowing me to illustrate and discuss his models, Dr. A. J. Kalnajs for his critical reading of an earlier version of this manuscript and for helpful discussions and insights, and the referee, Dr. J. Kormendy, who made many helpful comments and criticisms. I am also grateful to the Royal Greenwich Observatory and the European Southern Observatory for allowing me to reproduce images from their excellent survey charts. This work is based in part on my dissertation research.

REFERENCES

Athanassoula, E., Bosma, A., Crézé, M., and Schwarz, M. P. 1982, *Astr. Ap.*, **107**, 101.
Binggelli, B. 1980, *Astr. Ap.*, **82**, 289.
Buta, R. 1984*a*, *Univ. Texas Pub. Astr.*, No. 23.
_____. 1984b, *Proc. Astr. Soc. Australia*, **5**, 472.
Buta, R. 1986, *Ap. J. Suppl.*, **61**, 631 (Paper II).
Buta, R., and de Vaucouleurs, G. 1982, *Ap. J. Suppl.*, **48**, 219.
_____. 1983*a*, *Ap. J. Suppl.*, **51**, 149.
_____. 1983*b*, *Ap. J.*, **266**, 1.
Curtis, H. D. 1918, *Pub. Lick Obs.*, **13** (Part 1), 12.

Danby, J. M. A. 1965, *A.J.*, **70**, 501.
de Vaucouleurs, G. 1956, *Mem. Com. Obs. Mt. Stromlo*, vol. 3, No. 13.
_____. 1959, *Handbuch der Physik*, **53**, 275.
_____. 1963, *Ap. J. Suppl.*, **8**, 31.
_____. 1973, *Ap. J.*, **181**, 31.
_____. 1974, in *IAU Symposium 58, The Formation and Dynamics of Galaxies*, ed. J. R. Shakeshaft (Dordrecht: Reidel), p. 335.
_____. 1975, *Ap. J. Suppl.*, **29**, 193.
de Vaucouleurs, G., and Buta, R. 1980*a*, *A.J.*, **85**, 637 (deVB).
_____. 1980*b*, *Ap. J. Suppl.*, **44**, 451.
de Vaucouleurs, G., and de Vaucouleurs, A. 1964, *Reference Catalogue of Bright Galaxies* (Austin: University of Texas Press) (RC1).
Elmegreen, B. G., and Elmegreen, D. M. 1985, *Ap. J.*, **288**, 438.
Freeman, K. C., and de Vaucouleurs, G. 1974, *Ap. J.*, **194**, 569.
Gallagher, J. S., and Wirth, A. 1980, *Ap. J.*, **241**, 567.
Katz, N., and Richstone, D. O. 1984, *A.J.*, **89**, 975.
Kormendy, J. 1979, *Ap. J.*, **227**, 714.
_____. 1981, in *The Structure and Evolution of Normal Galaxies*, ed. S. Michael Fall and D. Lynden-Bell, (Cambridge: Cambridge University Press), p. 85.
_____. 1982*a*, in *Morphology and Dynamics of Galaxies* (Geneva: Geneva Observatory), p. 115.
_____. 1982*b*, *Ap. J.*, **257**, 75.
Lynds, R., and Toomre, A. 1976, *Ap. J.*, **209**, 382.
Miller, R. H. 1978, *Ap. J.*, **226**, 81.
O'Connell, R. W., Scargle, J. D., and Sargent, W. L. W. 1974, *Ap. J.*, **191**, 61.
Pedreros, M., and Madore, B. F. 1981, *Ap. J. Suppl.*, **45**, 541.
Peterson, C. J. 1982, *Pub. A.S.P.*, **94**, 409.
Sandage, A. 1961, *The Hubble Atlas of Galaxies* (*Carnegie Inst. Washington Pub.*, No. 618).
_____. 1975, in *Stars and Stellar Systems*, Vol. 9, *Galaxies and the Universe*, ed. A. Sandage, M. Sandage, and J. Kristian (Chicago: University of Chicago Press), p. 1.
Sandage, A., and Brucato, R. 1979, *A.J.*, **84**, 472.
Sandage, A., and Tammann, G. A. 1981, *A Revised Shapley-Ames Catalog of Bright Galaxies* (*Carnegie Inst. Washington Pub.* No. 635) (RSA).
Schommer, R. A. 1976, *Bull. AAS*, **8**, 314.
Schwarz, M. P. 1979, Ph.D. thesis, Australian National University.
_____. 1981, *Ap. J.*, **247**, 77.
_____. 1984*a*, *Astr. Ap.*, **133**, 222.
_____. 1984*b*, *M.N.R.A.S.*, **209**, 93.
_____. 1984*c*, *Proc. Astr. Soc. Australia*, **5**, 458.
_____. 1985, *M.N.R.A.S.*, **212**, 677.
Schweizer, F. 1980, *Ap. J.*, **237**, 303.
Schweizer, F., Whitmore, B., and Rubin, V. C. 1983, *A.J.*, **88**, 908.
Sersic, J. L. 1958, *Observatory*, **78**, 125.
Simkin, S. M., Su, H. J., and Schwarz, M. P. 1980, *Ap. J.*, **237**, 404.
Stark, A. A. 1977, *Ap. J.*, **213**, 368.
Theys, J. C., and Spiegel, E. A. 1976, *Ap. J.*, **208**, 650.

R. BUTA: Mount Stromlo Observatory, Private Bag, Woden P.O., Canberra, ACT 2606, Australia